國 立 交 通 大 學

電信工程學系碩士班

碩士論文

協力式多樣技術於 WiMAX OFDM(A)系統之運用

Incorporation of Cooperative Diversity in WiMAX OFDM(A) Based Systems

研 究 生：廖晨吟　　Student: Chen-Yin Liao

指導教授：李大嵩 博士　　Advisor: Dr. Ta-Sung Lee

中 華 民 國 九 十 七 年 六 月

協力式多樣技術於 WiMAX OFDM(A)系統之運用

Incorporation of Cooperative Diversity in WiMAX OFDM(A) Based Systems

研 究 生：廖晨吟　　Student: Chen-Yin Liao

指導教授：李大嵩 博士　　Advisor: Dr. Ta-Sung Lee

國立交通大學

電信工程學系碩士班

碩士論文

A Thesis
Submitted to Department of Communication Engineering
College of Electrical and Computer Engineering
National Chiao Tung University
in Partial Fulfillment of the Requirements
for the Degree of
Master of Science
in
Communication Engineering
June 2008
Hsinchu, Taiwan, Republic of China

中 華 民 國 九 十 七 年 六 月

協力式多樣技術於 WiMAX OFDM(A)系統之運用

學生：廖晨吟　　指導教授：李大嵩 博士

國立交通大學電信工程學系碩士班

摘要

正交分頻多工系統為新一代無線通訊系統最常使用的技術，如 IEEE 802.11a/g/n、 IEEE 802.16、IEEE 802.20、數位電視、數位廣播等許多系統均採用此技術。協力式多樣傳輸為近年來無線通訊系統中被廣泛討論的新技術，其概念為利用中繼節點幫助傳送以有效提升系統整體效能。在本論文中，吾人首先設計出兩種協力式多樣傳送的機制來有效執行協力式多樣傳輸，並且推導兩種機制的錯誤率上界，並以數學模型趨近表示之。吾人在第二部份中，提出在適應性調變編碼和適應性天線系統的支援下，能讓協力式傳輸更有效改善整體效能的機制。最後吾人以 IEEE 802.16(e)正交分頻多工存取的訊框結構為範例，提出一連結適應機制，藉由在基地台進行協力式傳送的評估，並且決定最佳之傳送機制，可有效使整體系統吞吐量優於傳統的直接傳送方式。吾人藉由電腦模擬驗證提出之新連結適應法以及上述在低速移動的 IEEE 802.16-2005 環境規格下，可有效改善位元錯誤率和整體系統吞吐量。

Incorporation of Cooperative Diversity in WiMAX OFDM(A) Based Systems

Student: Chen-Yin Liao Advisor: Dr. Ta-Sung Lee

Department of Communication Engineering

National Chiao Tung University

Abstract

Orthogonal Frequency Division Multiplexing (OFDM) is a popular technique in modern wireless communications. There are many systems adopting the OFDM technique, such as IEEE 802.11 a/g/n, IEEE 802.16, Digital Video Broadcasting, etc. Cooperative transmission is a new and promising technique in wireless communication systems, and it can improve the end-to-end throughput of the system by introducing relay terminals into networks. We propose two cooperative diversity schemes to efficiently incorporate the cooperative transmission in OFDM(A) based systems, and derive the BER upper bounds of two schemes. In order to make the overall performance of cooperative transmission better, the modified cooperative diversity schemes are proposed to employ cooperative transmission to AAS and AMC zones. At last, we propose a link adaptation method in OFDMA frame structure. The proposed link adaptation method is for base stations to evaluate the performance of each transmission scheme and choose the one which can provide the highest throughput. We evaluate the performance of the proposed system under slow mobility using IEEE 802.16-2005 standard and confirm that it achieves good performance.

Acknowledgement

I would like to express my deepest gratitude to my advisor, Dr. Ta-Sung Lee, for his enthusiastic guidance and great patience. I also wish to thank my friends for their encouragement and help. Finally, I would like to show my sincere thanks to my parents for their inspiration and love.

Contents

List of Figures

List of Tables

Acronym Glossary

3GPP	third generation partnership project
AAS	Adaptive Antenna System
AF	amplify-and-forward
AMC	Adaptive Modulation and Coding
AOA	angle of reception
AOD	angle of departure
AWGN	additive white Gaussian noise
BS	base station
CCIR	co-channel interference rejection
CINR	carrier-to-interference-and-noise ratio
Coop-MISO	cooperative MISO scheme
Coop-SIMO	cooperative SIMO scheme
CRC	cyclic redundancy check
DF	decode-and-forward
DL	downlink
DFT	discrete fourier transform
FEC	forward error correction
FFT	fast fourier transform
FUSC	Full Usage of Subchannels
IEEE	institute of electrical and electronics engineers

IDFT	inverse discrete fourier transform
IFFT	inverse fast fourier transform
ISI	inter-symbol interference
LOS	line-of-sight
MISO	multiple-input-single-output
MRC	maximum ratio combining
MS	mobile station
NLOS	non-line-of-sight
OFDM	orthogonal frequency division multiplexing
OFDMA	orthogonal frequency division multiple access
PUSC	Partial Usage of Subchannels
QAM	quadrature amplitude modulation
QOS	quality of service
QPSK	quadrature phase shift keying
SIMO	single-input-multiple-output
SNR	signal-to-noise ratio
STC	space time coding
TDD	time division duplexing
UL	uplink
WiMAX	worldwide interoperability for microwave access

Notations

BW	bandwidth
N	FFT size
L_{cp}	sample numbers of cyclic prefix
H	channel frequency response
h	channel time response
g	multipath channel tap gain
τ	multipath delay
x	time domain transmit signal
X	frequency domain transmit signal
y	time domain receive signal
Y	frequency domain receive signal
P	pilot magnitude
N_d	number of subcarriers used for data transmission
N_g	number of subcarriers used for guard band
N_p	number of subcarriers used for data transmission
T_s	sampling time

Chapter 1

Introduction

Wireless communication systems have been in use for quite a long time. Many standards are available based on which user devices communicate, but the present standards fail to provide sufficient data rate, and broadband wireless access is an appealing way to provide flexible and easily-to-deploy solution. In view of this requirement for future mobile wireless communication systems, the 802.16 standard has been proposed by Institute of Electrical and Electronic Engineers (IEEE) [1], [2].

The WiMAX (Worldwide Interoperability for Microwave Access) Forum is committed to providing optimized solutions for fixed, nomadic, portable and mobile broadband wireless access. Two versions of WiMAX address the demand for these different types of access:

• **IEEE 802.16-2004:** This is based on the 802.16-2004 version of the IEEE 802.16 standard. It uses Orthogonal Frequency Division Multiplexing (OFDM) and supports fixed and nomadic access in Line of Sight (LOS) and Non Line of Sight (NLOS) environments. For LOS environment, the frequency range in 802.16d is from 2GHz to 66GHz and Single Carrier (SC) is mainly adopted as the transmission scheme. For NLOS environment, it focuses on the Broadband Wireless Access (BWA), where the frequency band ranges from 2GHz to 10GHz. In physical layer (PHY), NLOS temps to adopt OFDM and OFDMA techniques.

• **IEEE 802.16-2005:** Optimized for dynamic mobile radio channels. This version is based on the IEEE 802.16-2005 amendment and provides support for handoffs and roaming. The choice of the subcarrier number becomes more flexible since it provides four options, 128, 512, 1024, and 2048. The frequency band ranges from 2GHz to 6GHz.

Orthogonal Frequency Division Multiplexing (OFDM) is a popular technique in modern wireless communication systems. In an OFDM system, the bandwidth is divided into several orthogonal subchannels for transmission. A cyclic prefix (CP) is inserted before each symbol. Therefore, if the delay spread of the channel is shorter than the length of the cyclic prefix, the intercarrier symbol interference (ISI) can be eliminated due to the cyclic prefix. On the other hand, subcarriers in OFDM are orthogonal to each other over time-invariant channels, so the conventional OFDM system only requires one-tap equalizers [3] to compensate the channel response. This characteristic simplifies the design of the OFDM receiver, and for this reason, the OFDM technique is widely used in wireless communication systems.

Future wireless networks will be highly dynamic with extreme demands on performance, especially in terms of bandwidth and energy. The use of multiple antennas can provide significant improvement in power and spectral efficiency in wireless communications. However, it might be impractical in many cases due to the limited size and power of the terminals. By exploiting the broadcast nature of the wireless networks, a virtual MIMO system can be realized through cooperation among nodes [4-6]. Cooperative diversity has recently emerged as a promising alternative to combat fading in wireless channels. The fundamental idea is that nodes in a wireless network share their information and transmit cooperatively as a virtual antenna array, thus providing diversity without the requirement of additional antennas at each node. In [7], the authors proposed some cooperative strategies including fixed

relaying, selection relaying, and incremental relaying schemes. In [8], user cooperation diversity was proposed for CDMA system in which orthogonal codes are used to mitigate multiple access interference.

In the simplest embodiment of cooperative networking, some nodes may simply relay a message [9]. This type of relaying has been proposed to augment the performance of infrastructure-based networks, such as WiMAX. Since cooperation is a promising architecture for next generation wireless system and OFDM is one of the most popular physical-layer technologies for wireless systems, the combination of the two techniques named OFDM-relay will be a good candidate technology for future wideband wireless communications.

The rest of this thesis is organized as follows. In Chapter 2, an overview of WiMAX system is given. The transmit techniques such as Space-Time Coding (STC), Adaptive Antenna System (AAS), Adaptive Modulation and Coding (AMC) are also introduced. In Chapter 3, two cooperative diversity schemes are proposed and the average BER upper bounds are derived. In Chapter 4, we modify cooperative diversity schemes to match up the properties of AAS and AMC, and propose a link adaptation method for the base station to determine the transmission schemes. Several computer simulation results are also given to show the performance improvement of the proposed cooperative diversity schemes in IEEE 802.16-2005 system. In Chapter 5, we conclude this thesis and future work can be the design of the proposed link adaptation method for users with high speeds.

Chapter 2

Overview of WiMAX System

WiMAX is a broadband wireless technology that supports fixed, nomadic, portable and mobile access. To meet the requirements of different types of access, two versions of WiMAX have been defined. The first is based on IEEE 802.16-2004 and is optimized for fixed and nomadic access. The second version is designed to support portability and mobility, and will be based on the IEEE 802.16-2005 amendment to the standard. In this chapter, we will focus on the physical layer of orthogonal frequency division multiplexing (OFDM) and orthogonal frequency division multiple access (OFDMA) structure in IEEE 802.16-2005. Then, the transmit techniques such as STC and AAS adopted in the system will be introduced. Finally, the channel model for fixed wireless application will be mentioned.

2.1 Physical Layer Description

Worldwide Interoperability of Microwave Access (WiMAX) is a broadband wireless technology that supports fixed, nomadic, portable and mobile access. In other words, WiMAX is a technology based on the IEEE 802.16 specifications to enable the delivery of last mile wireless broadband access as an alternative to cable and DSL. WiMAX will provide wireless broadband connectivity without the requirement for

direct line-of-sight (LOS) with a base station. WiMAX provides metropolitan area network connectivity at speeds of up to 75 Mb/sec, and WiMAX systems can be used to transmit signal as far as 30 miles. However, on the average a WiMAX base-station installation will likely cover between three to five miles [10].

WiMAX covers both LOS and NLOS applications in the 2-66 GHz frequencies. The PHY layer contains several forms of multiplexing and modulation to support different frequency range and application. Data rates determined by exact modulation and encoding schemes are shown in Table 2-1. The IEEE 802.16 standard was originally written to support several physical medium interfaces and it is expected that it will continue to develop and extend to support other PHY specifications. Hence, the modular nature of the standard is helpful in this aspect. For example, the first version of the standard only supported single carrier modulation. Since that time, OFDM has been added [11].

Table 2-1: Data rate for different modulations and code rates

Bandwidth (MHz)	Raw bit rate (Mb/s)		
	QPSK, CC3/4	**16QAM, CC3/4**	**64QAM, CC3/4**
6	7.5	15	22.5
7	8.7	17.5	26.1
20	24.4	48.8	73.2

In IEEE 802.16-2005, its applications are focused on mobile applications in the 2-6 GHz. Two multi-carrier modulation techniques are supported in 802.16-2005: OFDM with 256 carriers and OFDMA with 128, 512, 1024, or 2048 carriers.

In the following sections, we will introduce the main block diagrams of the transmitter architecture. We will focus on physical layer description on OFDM and OFDMA mode in IEEE 802.16-2005.

2.1.1 Randomizer

The randomization is performed on each burst of data on the DL and UL, which means that for each allocation of a data block, the randomizer shall be used independently. For RS and CC encoded data, padding will be added to the end of the transmission block, up to the amount of data allocated minus one byte, which shall be reserved for the introduction of a 0x00 tail byte by the FEC. The PRBS generator shall be $1+X^{14}+X^{15}$ as shown in Figure 2-1. Each data byte to be transmitted shall enter sequentially into the randomizer. Preambles are not randomized.

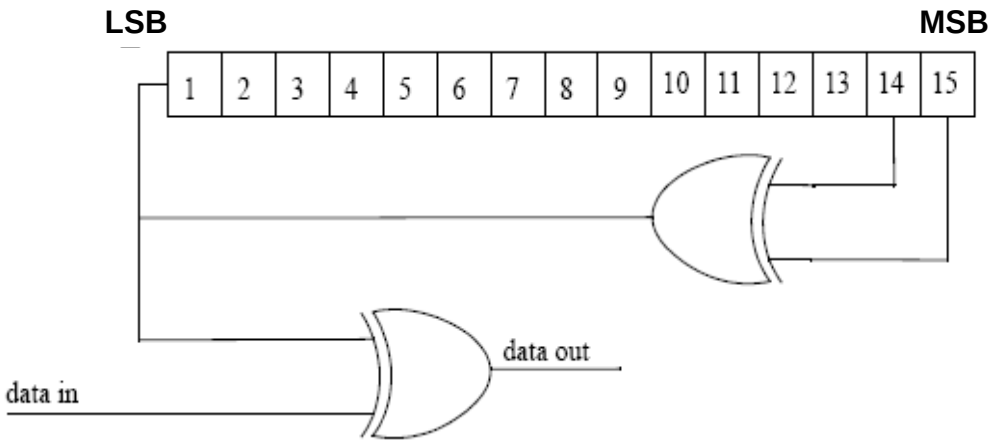

Figure 2-1: PRBS generator for randomizer

On the downlink, the randomizer shall be re-initialized at the start of each frame. In OFDMA mode, the randomizer shall be re-initialized with the sequence: [LSB]011011100010101[MSB]. At the start of subsequent bursts, the randomizer shall be initialized with the vector shown in Figure 2-2. The frame number used for initialization refers to the frame in which the DL burst is transmitted. The subchannel offset used for initialization refers to the allocated subchannels in which the DL burst is transmitted.

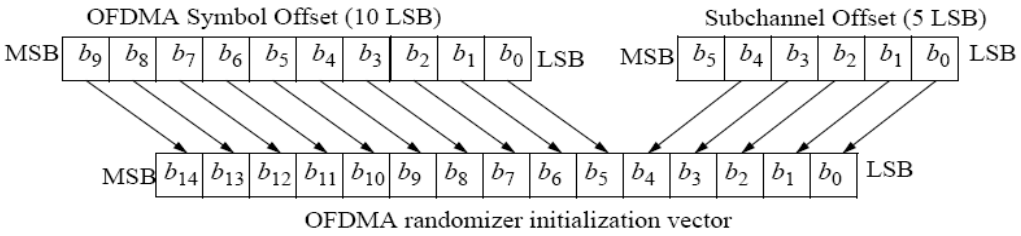

Figure 2-2: OFDMA randomizer DL initialization vector

2.1.2 Forward Error Correction

The encoding is performed by passing the data in block format through a convolutional encoder. A single 0xFF tail byte is appended to the end of each burst after randomization. Each data block is encoded by the binary convolutional encoder, which shall have native rate of 1/2, a constraint length equal to 7, and shall use the generator depicted in Figure 2-3. Puncturing patterns and serialization order that shall be used to realize different code rates are defined in Table 2-2. Table 2-3 gives the data payload sizes and the code rates used for the different modulations.

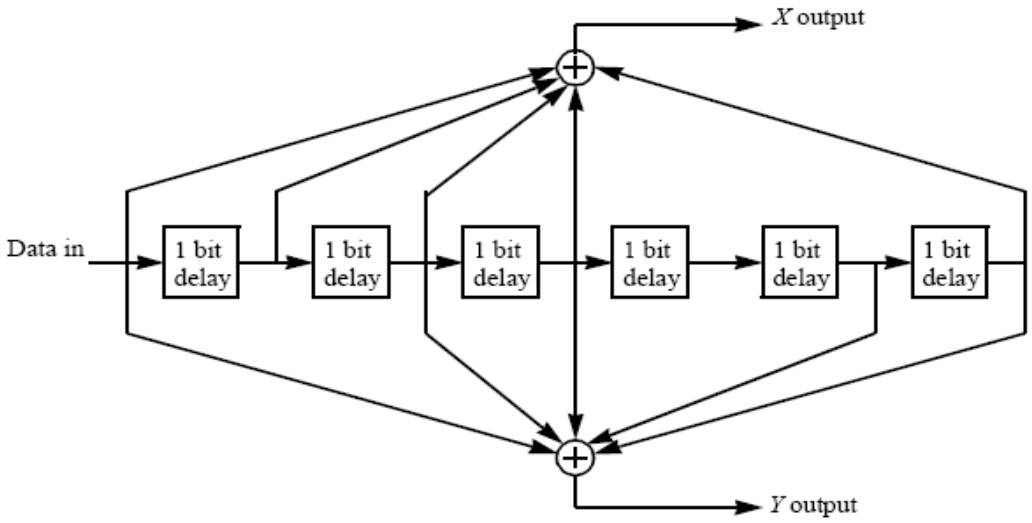

Figure 2-3: Convolutional encoder

Table 2-2: Puncturing patterns and orders to realize different code rates

	Code rates		
Rate	$1/2$	$2/3$	$3/4$
d_{free}	10	6	5
X	1	10	101
Y	1	11	110
XY	$X_1 Y_1$	$X_1 Y_1 Y_2$	$X_1 Y_1 Y_2 X_3$

Table 2-3 Useful data payload for a slot

	QPSK		16 QAM		64 QAM		
Encoding rate	R=1/2	R=3/4	R=1/2	R=3/4	R=1/2	R=2/3	R=3/4
Data payload (bytes)	6						
		9					
	12		12				
	18	18		18	18		
	24		24			24	
		27					27
	30						
	36	36	36	36	36		

2.1.3 Interleaver

After FEC, all encoded data bits shall be interleaved by a block interleaver with a block size corresponding to the number of coded bits over the allocated subchannels per OFDM symbol. The interleaver is defined by two step permutation. The first permutation ensures that adjacent coded bits are mapped onto nonadjacent subcarriers. The second permutation ensures that adjacent coded bits are mapped alternately onto less or more significant bits of the constellation, thus avoiding long runs of lowly reliable bits.

2.1.4 Modulator

The data are entered serially to the constellation mapper after interleaving. In OFDMA mode, Gray-mapped QPSK, 16QAM, and 64QAM shall be supported. The constellation-mapped data shall be subsequently modulated onto all allocated data subcarriers and each subcarrier multiplied by the factor $2*(1/2-w_k)$ according the subcarrier index, *k*.

Pilot Modulation

Pilot subcarriers shall be inserted into each data burst in order to constitute the symbol and they shall be modulated according to their carrier location within the symbol. The PRBS generator depicted in Figure 2.4 shall be used to produce a sequence, w_k. The polynomial for the PRBS generator shall be $1+X^9+X^{11}$. For OFDMA mode, each pilot shall be transmitted with a boosting of 2.5 dB over the average power of each data tone. The pilot subcarriers shall be modulated according to (2-1):

$$\mathrm{Re}\{c_k\} = \frac{8}{3}(\frac{1}{2}-w_k) \quad \text{and} \quad \mathrm{Im}\{c_k\} = 0. \tag{2-1}$$

The pilot in DL preamble shall be modulated according to (2-2):

$$\begin{aligned} \mathrm{Re}\{premablePilotsModulated\} &= 4\cdot\sqrt{2}\cdot(\frac{1}{2}-w_k) \\ \mathrm{Im}\{premablePilotsModulated\} &= 0 \end{aligned} \tag{2-2}$$

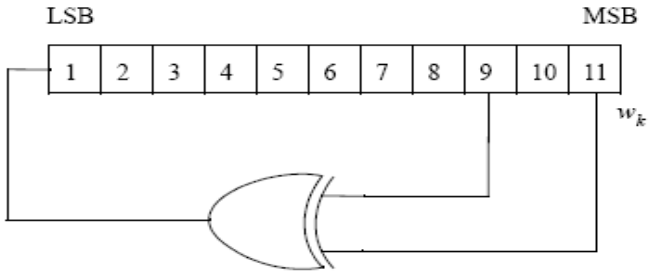

Figure 2-4: PRBS generator for pilot modulation

Preamble Structure

The first symbol of the DL transmission is the preamble and the preamble subcarriers are divided into three carrier-sets. Those subcarriers are modulated using a boosted BPSK modulation with a specific PN code. There are three possible groups consisting of a carrier-set each that may be used by any segment. Each segment uses a preamble composed of a carrier-set out of the three available carrier-sets in the following manner: (In the case of segment 0 under 2048-FFT, the DC carrier will not be modulated at all and the appropriate PN will be discarded; therefore, DC carrier shall be always zero. For the preamble symbol of 2048-FFT, there will be 172 guard band subcarriers on the left side and the right side of the spectrum). For example, Figure 2-8 depicts the preamble of segment 1 for 2048-FFT.

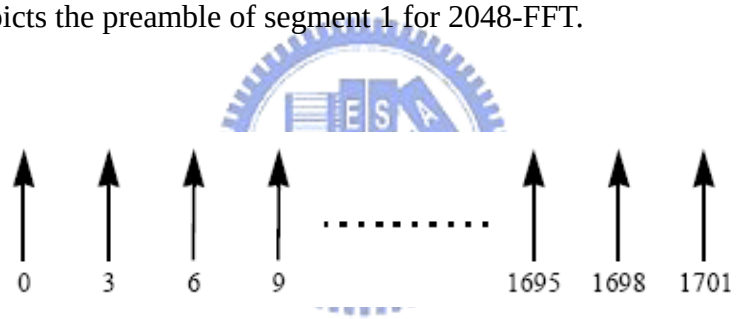

Figure 2-5: Example of DL preamble for segment 1

2.2 Key Features of Scalable OFDMA

Scalable OFDMA (SOFDMA) is IEEE 802.16-2005 enhanced physical layer and it includes many important features for fixed, nomadic, and mobile networks. Because of these advantages, most of the industry will build their IEEE 802.16-2005 products using SOFDMA technology. However, the IEEE 802.16-2005 standard is not just for mobility. There are also many compelling reasons for using SOFDMA in fixed broadband wireless access (BWA) networks. In this section, we will focus on some key features of SOFDMA for wireless applications [12], [13].

2.2.1 Scalable Channel Bandwidth

Scalability is one of the most important advantages of OFDMA. Spectrum resources for wireless broadband worldwide are still quite different in its allocation. With OFDMA subcarrier structure, it is designed to be able to scale to work in different channelization from 1.25 to 20 MHz to cope with varied worldwide requirements as efforts proceed to achieve spectrum harmonization in the longer term. The scalability is supported by adjusting FFT size according to the different channel bandwidth to fix the subcarrier frequency spacing. By fixing the subcarrier spacing and symbol duration, the basic unit of physical resource is fixed. Therefore, the impact to higher layers is minimal when scaling the bandwidth.

The significant advantage from scalability is the flexibility of deployment. With the little modification to different air interfaces, OFDMA system can be deployed in various frequency bands to flexibly address the requirement for various spectrum allocation and usage model requirements. The OFDMA scalability parameters used in the thesis are listed in Table 2-4. The subcarrier spacing is fixed to 11.16 kHz and the symbol time is fixed to 89.6 μs . With the flexibility to support wider range bandwidth, OFDMA also enjoys high sector throughput, which allows more efficient multiplexing of data traffic, lower latency and better quality of service (QoS).

Table 2-4: OFDMA scalability parameters for different bandwidth

Parameters	Values				
Bandwidth (MHz)	1.25	2.5	5	10	20
Sampling frequency (MHz)	1.43	2.86	5.71	11.4	22.8
FFT size	128	256	512	1024	2048
Subcarrier spacing	11.16 KHz				
Useful symbol time (Tb)	89.6 us				
CP duration	22.4 us (Tb/4)				

2.2.2 Sub-channelization and Permutation

Active (data and pilot) subcarriers are grouped into subsets of subcarriers called subchannels. The OFDMA PHY supports sub-channelization in both DL and UL. The minimum frequency-time resource unit of sub-channelization is one slot, which is equal to 48 data tones. There are two major types of subcarriers permutation for subchannelization: diversity and contiguous. The diversity permutation takes subcarriers pseudo-randomly to form a subchannel. The diversity permutations include DL & UL PUSC (Partial Usage of Subchannels), DL FUSC (Full Usage of Subchannels), and additional optional permutations. The contiguous permutation groups a block of adjacent sub-carriers to form a subchannel. The contiguous permutations include DL & UL AMC (Adaptive Modulation and Coding). With DL PUSC, for each pair of OFDM symbols, the usable subcarriers are grouped into *clusters* containing 14 adjacent subcarriers per symbol, with pilot and data allocations in each cluster in the even and odd symbols as shown in Figure 2-6. Other definitions of the PUSC subcarrier allocation are: one *subchannel* contains two clusters by one OFDMA symbol and one *slot* is one subchannel by two OFDMA symbols.

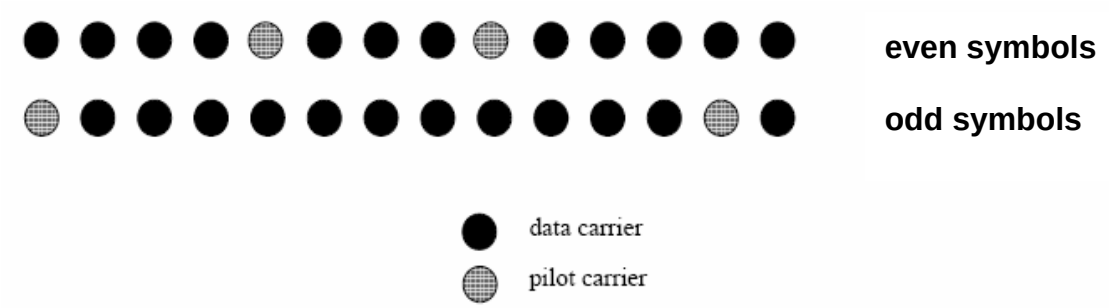

Figure 2-6: Cluster structure

Divide these clusters into several Major Groups. The allocation algorithm varies with FFT sizes. For each subchannel, subcarriers are distributed in some clusters that belong to its major group as shown in Figure 2.7. A subchannel contains 2 clusters and is comprised of 48 data subcarriers and 8 pilot subcarriers. Allocating subcarriers to subchannel in each major group is performed separately for each OFDMA symbol by first allocating the pilot carriers within each cluster, and then taking all remaining data carriers within the symbol and using the procedure described in (2-3):

$$subcarrier(k,s) = N_{subchannels} \cdot n_k + \{p_s[n_k \bmod N_{subchannels}] + DL\_PermBase\} \bmod N_{subchannels}, \quad (2\text{-}3)$$

where

$subcarrier(k,s)$ is the subcarrier index k in subchannel s

$N_{subchannels}$ is the number of subchannels in current partitioned major group

$n_k = (k + 13 \cdot s) \bmod N_{subccarriers}$

$N_{subccarriers}$ is the number of data subcarriers allocated to a subchannel

$p_s[j]$ is the series obtained by rotating basic permutation sequence cyclically to the left s times

The parameters vary with FFT sizes. Figure 2-8 shows an example of mapping OFDMA slots into subchannels and symbols in the DL PUSC.

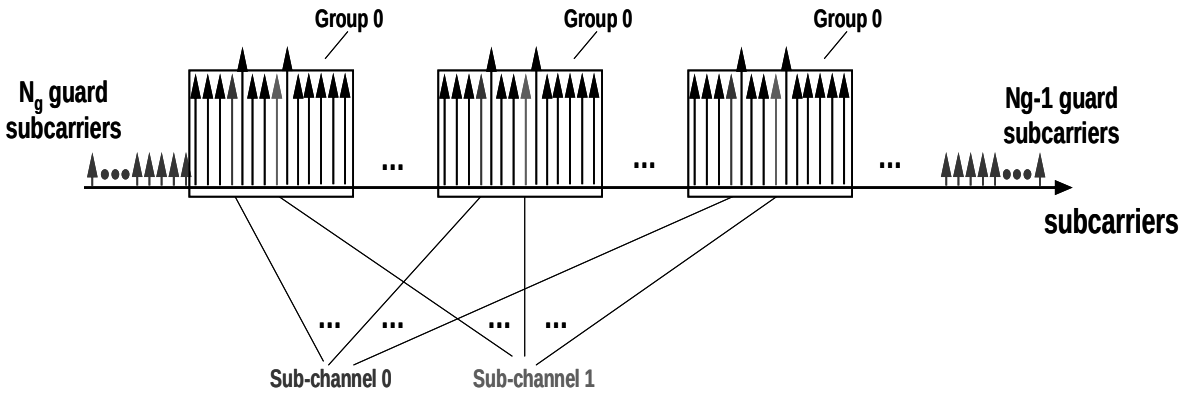

Figure 2-7: Allocated subcarriers into subchannels for PUSC

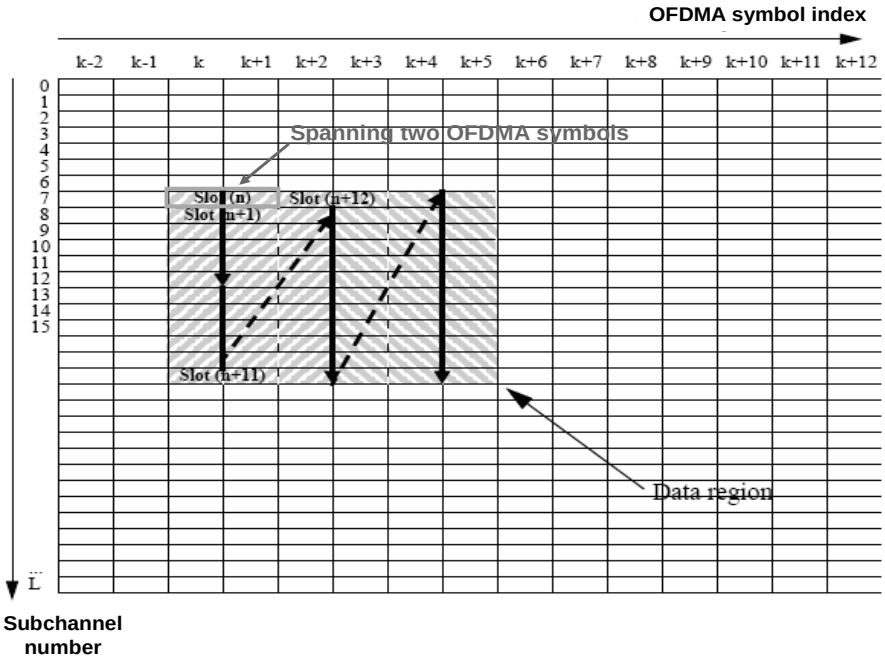

Figure 2-8: Example of mapping OFDMA slots to subchannels and symbols in DL PUSC

Compared with the cluster structure for DL PUSC, a *tile* structure is defined for the UL PUSC whose format is shown in Figure 2-9. The slot is comprised of 48 data subcarriers and 24 pilot subcarriers in 3 OFDM symbols.

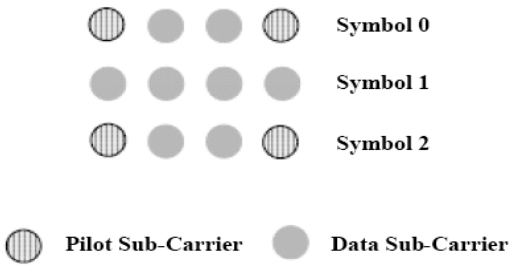

Figure 2-9: Description of a UL PUSC tile

FUSC achieves full diversity by spreading tones over entire band. The symbol structure is constructed using pilots, data, and zero subcarriers. The symbol is first allocated with the appropriate pilots and with zero subcarriers, and then all the remaining subcarriers are used as data subcarriers. To allocate the data subchannels, the remaining subcarriers are partitioned into groups of contiguous subcarriers. Each subchannel consists of one subcarrier from each of these groups as shown in Figure 2-10. The number of groups is therefore equal to the number of subcarriers per subchannel. The exact partitioning into subchannels is according to the same procedure as (2-3).

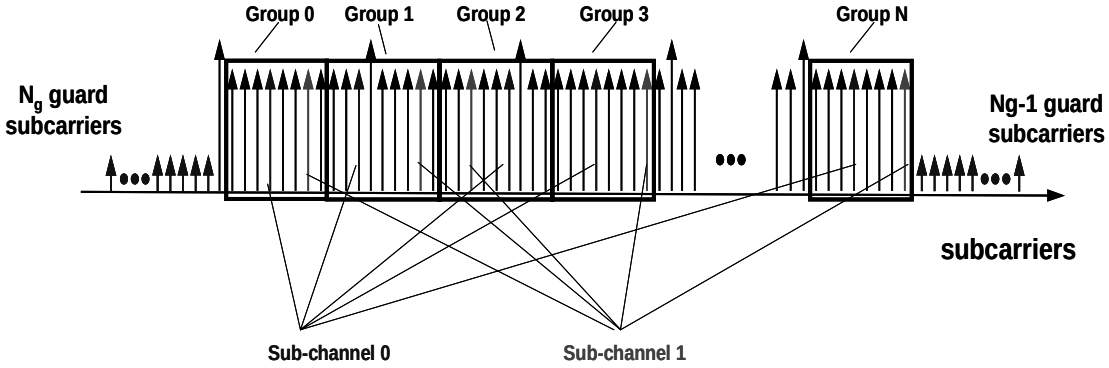

Figure 2-10: Allocated subcarriers into subchannels for FUSC

The contiguous permutation groups a block of adjacent subcarriers to form a subchannel, such as DL AMC and UL AMC. As shown in Figure 2-11, a bin consists

of nine adjacent subcarriers in a symbol, with eight tones for data and one assigned for a pilot. A *slot* in AMC is defined as a collection of bins of the type (N x M = 6), where N is the number of adjacent bins and M is the number of adjacent symbols. Thus 4 different ways of defining a slot are (6 bins, 1 symbol), (3 bins, 2 symbols), (2 bins, 3 symbols), (1 bin, 6 symbols). AMC permutation enables multi-user diversity by choosing the sub-channel with the best channel frequency response.

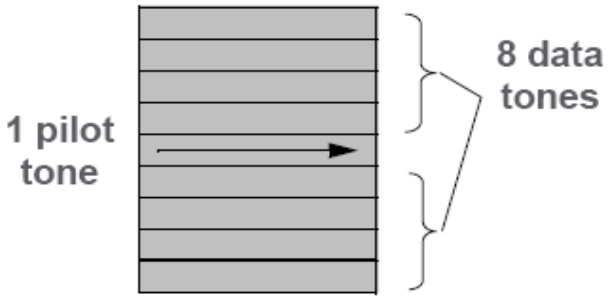

Figure 2-11: AMC bin structure

In general, diversity subcarrier permutations perform well in mobile applications while contiguous subcarrier permutations are well suited for fixed, portable, or low mobility environments. These options enable the system designer to trade-off mobility for throughput.

2.3 Transmit Techniques

To increase the converge and reliability of WiMAX systems, the WiMAX standard supports optional multiple-antenna techniques such as Alamouti Space-Time Coding (STC), Adaptive Antenna Systems (AAS) and Multiple-Input Multiple-Output (MIMO) systems.

There are several advantages to using multiple-antenna technology compared with single-antenna technology:

• **Array Gain:** This is the gain achieved by using multiple antennas so that the signal adds coherently.

• **Diversity Gain:** This is the gain achieved by utilizing multiple paths so that the probability that any one path is bad does not limit performance. Effectively, diversity gain refers to techniques at the transmitter or receiver to achieve multiple “looks” at the fading channel. These schemes improve performance by increasing the stability of the received signal strength in the presence of wireless signal fading. Diversity may be exploited in the spatial (antenna), temporal (time), or spectral (frequency) dimensions.

• **Co-channel Interference Rejection (CCIR):** This is the rejection of signals by making use of the different channel response of the interferers.

2.3.1 Transmit Diversity: Space-Time Coding

In order to increase the rate and range of the modem, there are several considerations. Generally, BS can bear more cost and complexity than SS, so multiple-antenna techniques are good option at BS, also called transmit diversity. Among various transmit diversity schemes, STC is the most popular scheme with the feature of open loop (i.e., no feedback signaling is required) as channel information is not required at the transmitter. Therefore we will focus on the scheme of STC with 2 transmit antennas in this section as shown in Figure 2-12.

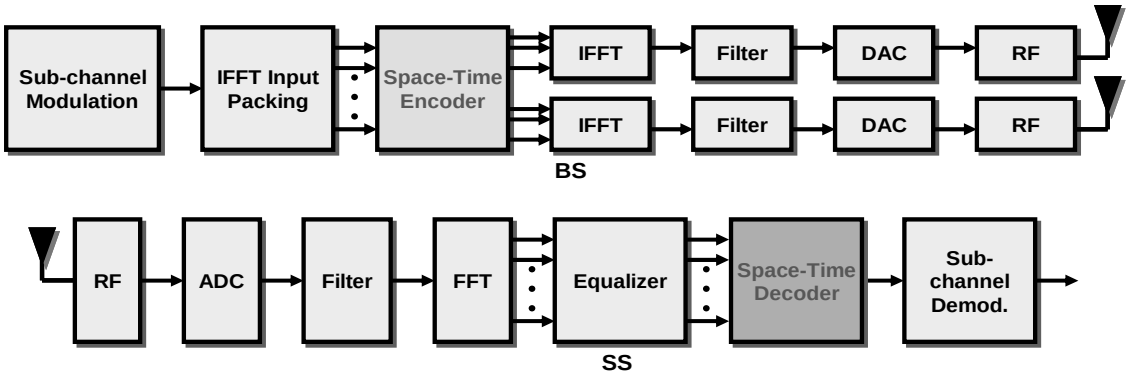

Figure 2-12: Block diagram of STC

The space-time block coding scheme was first discovered by Alamouti for two transmit antennas. Symbols transmitted from those antennas are encoded in both space and time in a simple manner to ensure that transmissions from both the antennas are orthogonal to each other. This would allow the receiver to decode the transmitted information with a slight increment in the computational complexity.

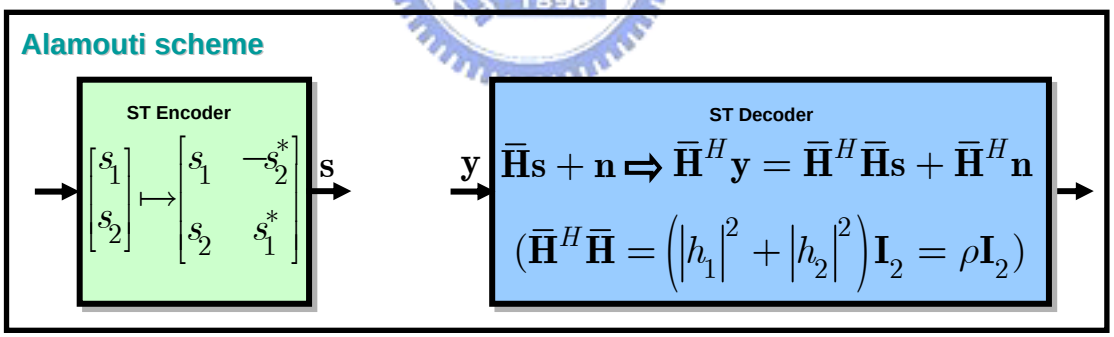

Figure 2-13: Illustration of Alamouti scheme

Figure 2-13 shows the operation of Alamouti scheme. The input symbols to the space-time block encoder are divided into groups of two symbols. At a given symbol period, the encoder takes a block of two modulated symbols s_1 and s_2 in each encoding operation and maps them to the transmit antennas according to a code matrix given by

$$\mathbf{s} = \begin{bmatrix} s_1 & -s_2^* \\ s_2 & s_1^* \end{bmatrix}. \tag{2-4}$$

The encoder outputs are transmitted in two consecutive transmission periods from two transmit antennas. Let h_1 and h_2 be the channel gains from the first and second transmit antennas to the only one receiver antenna. Assume that h_1 and h_2 are scalar and constant over two consecutive symbol periods. The received signals in two consecutive symbol periods, denoted as r_1 and r_2, can be expressed as

$$\begin{aligned} r_1 &= h_1 s_1 + h_2 s_2 + n_1 \\ r_2 &= -h_1 s_2^* + h_2 s_1^* + n_2, \end{aligned} \tag{2-5}$$

where n_1 and n_2 are AWGN noise modeled as identical independent distributed (i.i.d.) complex Gaussian random variables with zero mean and power spectral density $N_0/2$ for each dimension. The above equation can be rewritten in a matrix form as

$$\mathbf{r} = \begin{bmatrix} r_1 \\ r_2^* \end{bmatrix} = \underbrace{\begin{bmatrix} h_1 & h_2 \\ (h_2)^* & -(h_1)^* \end{bmatrix}}_{\overline{\mathbf{H}}} \underbrace{\begin{bmatrix} s_1 \\ s_2 \end{bmatrix}}_{\mathbf{s}} + \underbrace{\begin{bmatrix} n_1 \\ n_2^* \end{bmatrix}}_{\tilde{\mathbf{n}}} = \overline{\mathbf{H}} \cdot \mathbf{s} + \tilde{\mathbf{n}}. \tag{2-6}$$

Since the channel matrix $\overline{\mathbf{H}}$ is unitary, i.e. $\overline{\mathbf{H}}^H \overline{\mathbf{H}} = \rho \cdot \mathbf{I}_2$, where $\rho = |h_1|^2 + |h_2|^2$, the ML decoder can perform an MRC operation on the modified signal vector $\tilde{\mathbf{r}}$ given by

$$\begin{aligned} \tilde{\mathbf{r}} &= \overline{\mathbf{H}}^H \cdot \mathbf{r} = \rho \cdot \mathbf{s} + \underbrace{\overline{\mathbf{H}}^H \cdot \tilde{\mathbf{n}}}_{\tilde{\mathbf{n}}} \\ &= \rho \cdot \mathbf{s} + \tilde{\mathbf{n}} \end{aligned}. \tag{2-7}$$

Therefore, we can obtain the space-time decoded vector $\mathbf{s}$.

For OFDMA mode, STC coding is done on all data subcarriers that belong to an STC coded burst in the two consecutive OFDMA symbols. Pilot subcarriers are not encoded and are transmitted from either antenna 0 or antenna 1. In PUSC, the pilot

allocation to cluster is changed as shown in Figure 2-14. The pilot locations change in period of four symbols to accommodate two antennas transmission with the same estimation capability.

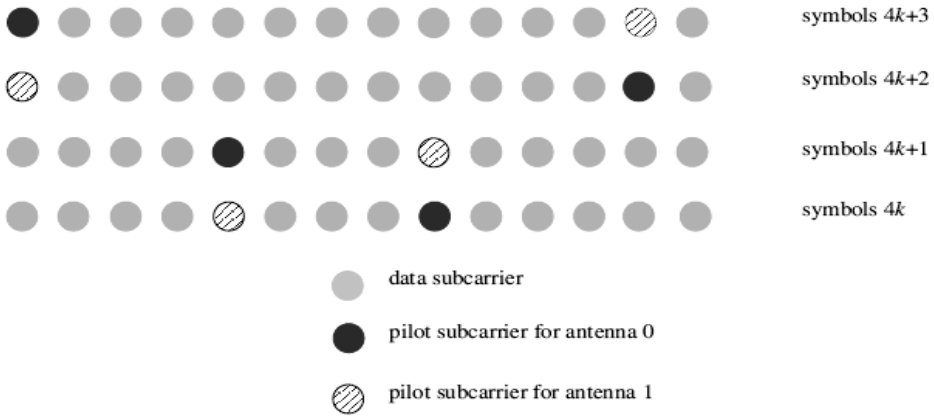

Figure 2-14: Cluster structure for STC PUSC using 2 Antennas

2.3.2 Transmit Beamforming: Adaptive Antenna System

Future wireless communication systems aim at providing higher data rates with better link quality subject to being interference limited. Smart antenna technology is one of the most promising technologies for increasing both system coverage and capacity as shown in Figure 2-15. AAS, although an optional feature, through the use of more than one antenna elements at BS, can significantly improve range and capacity by adapting the antenna pattern and concentrating its radiation to each individual user. There are several advantages of using beamforming:

- Increase spectral efficiency proportional to the number of antenna elements
- Realize an inter-cell frequency reuse of one and an in-cell reuse factor proportional to the number of antenna elements
- Reduce interference by steering nulls in directions of co-channel interferers

• Increase SNR of certain subscribers and steer nulls to others that can enable bursts to be concurrently transmitted to spatially separated users.

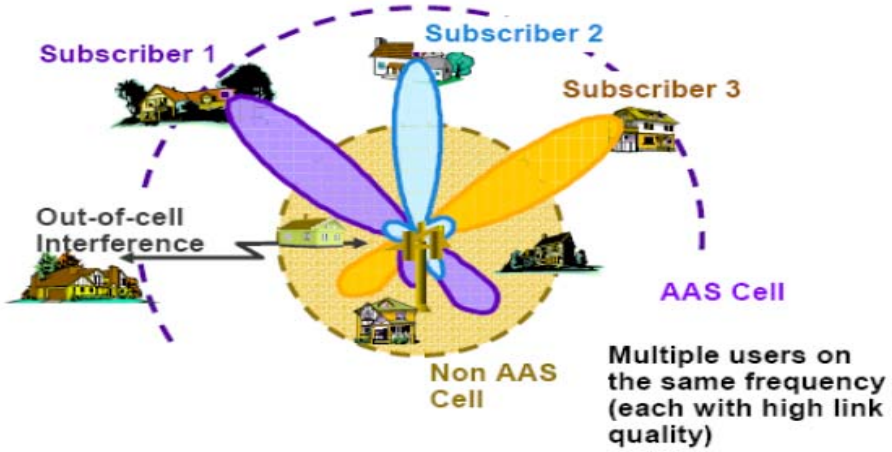

Figure 2-15: Illustration of AAS

First, the generalized AAS zone allocation is introduced as shown in Figure 2-16. The frame is divided into two parts: the fist part is allocated to the non-AAS users and the second part (called AAS zone) is allocated to the AAS users. This allows a mixture of non-AAS and AAS users to be supported by the same BS. The BS can dynamically allocate capacity to non-AAS and AAS traffic. The SS without AAS capability will ignore the traffic in the AAS zone.

Figure 2-17 shows the AAS zone structure in OFDMA mode. AAS_DLFP in an AAS zone is preceded by an AAS DL preamble of one symbol duration. All other data bursts within an AAS zone have a preamble whose duration is specified in AAS_DL_IE. AAS_DLFP provides a robust transmission of required BS parameters to enable SS access allocation. Each AAS_DLFP requires not carry the same information. Different beams may be used within the AAS diversity map zone. For

OFDMA mode, REP-RSP MAC message shall be sent by SS in response to a REP-REQ message from the BS to report estimation of the mean DL CINR (carrier-to-interference-and-noise ratio).

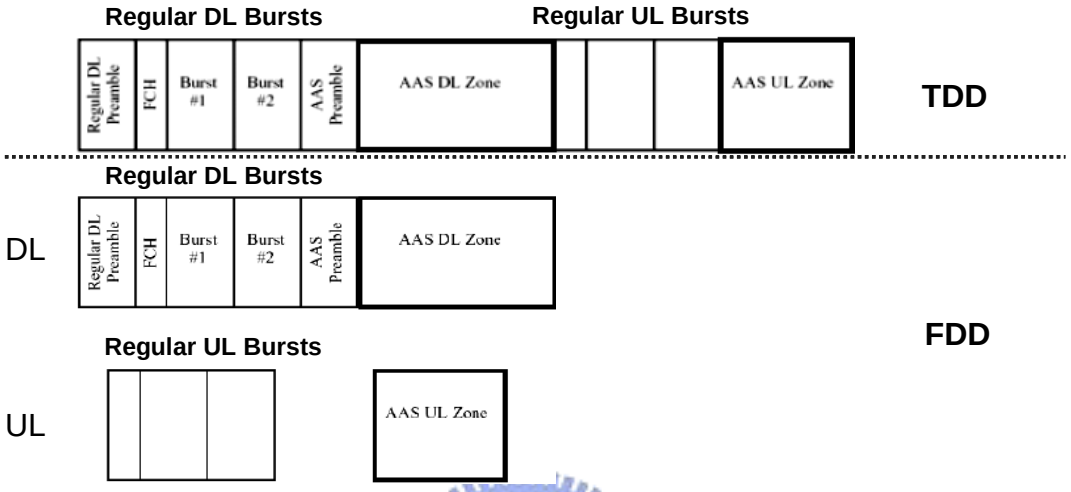

Figure 2-16: Generalized AAS zone allocation

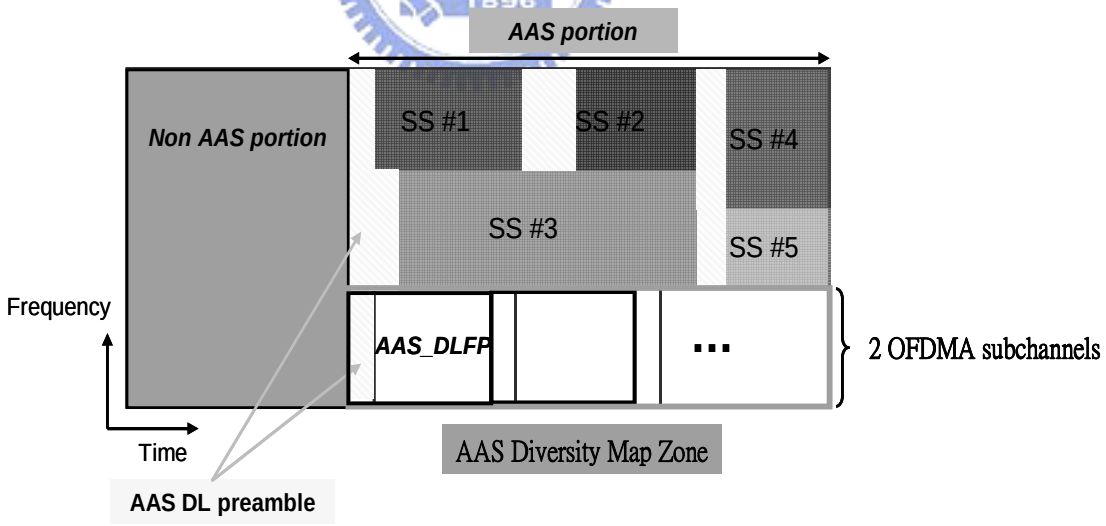

Figure 2-17: AAS zone structure in OFDMA mode

2.4 Channel Model

Wireless propagation channels have been studied for many years, and a large number of channel models are already available. The signal that has propagated

through a wireless channel consists of multiple echoes of the originally transmitted signals; this phenomenon is known as multipath propagation. The different multipath components are characterized by different attenuations and delays. The correct modeling of the parameters describing the multipath components is the key point of channel modeling.

In first generation systems, a super-cell architecture is used where the base station and subscriber station are in LOS condition and the system uses a single cell with no co-channel interference. For second generation systems, a scalable multi-cell architecture with NLOS conditions becomes necessary. In WiMAX system, the wireless channel is characterized by:

- Path loss (including shadowing)
- Multipath delay spread
- Fading characteristics
- Doppler spread

Because we consider mobile users with relatively low speed, the main channel model in our study is Stanford University Interim (SUI) channel models [14].

2.4.1 SUI Channel Model for Fixed Wireless Application

SUI channel models were proposed in [14] to model a statistic environment in IEEE 802.16-2004. There are many possible combinations of parameters to obtain different channel descriptions. A set of six typical channels were selected for the three terrain types that are typical of the continental US. The channel parameters are related to terrain type, delay spread, and antenna directionality and each channel model has three taps with distinct K-factor and average power. Table 2-5 shows an example of

time domain attribute of the SUI-3 channel, which is chosen to evaluate the performance.

Table 2-5: Parameters of SUI-3 channel models

SUI – 3 Channel				
	Tap 1	**Tap 2**	**Tap 3**	**Units**
Delay	0	0.4	0.9	μs
Power (omni ant.)	0	-5	-10	dB
90% K-fact. (omni)	1	0	0	
75% K-fact. (omni)	7	0	0	
Doppler	0.4	0.3	0.5	Hz
Antenna Correlation:	$\rho_{ENV} = 0.4$			
Gain Reduction Factor:	GRF = 3 dB			
Normalization Factor:	$F_{omni} = -1.5113$ dB, $F_{30°} = -0.3573$ dB			

Multipath Delay Profile

Due to the scattering environment, the channel has a multipath delay profile. It is characterized by τ_{rms} (RMS delay spread of the entire delay profile) which is defined as

$$\tau_{rms}^2 = \sum_j P_j \tau_j^2 - \left(\tau_{avg}\right)^2, \quad (2\text{-}8)$$

where

$\tau_{avg} = \sum_j P_j \tau_j$,

τ_j is the delay of the jth delay component of the profile and P_j is given by

P_j = (power in the jth delay component) / (total power in all components)

RMS delay spread

A delay spread model was based on a large body of published reports. It was found that the RMS delay spread follows lognormal distribution and that the median of this distribution grows as some power of distance. The model was developed for

rural, suburban, urban, and mountainous environments. The model is of the following form

$$\tau_{rms} = T_1 d^{\varepsilon} y \tag{2-9}$$

where τ_{rms} is the RMS delay spread, d is the distance in km, T_1 is the median value of τ_{rms} at d = 1 km, ε is an exponent that lies between 0.5 ~ 1.0, and y is a lognormal variant. Depending on the terrain, distance, antenna directivity and other factors, the RMS delay spread values can span from very small values (tens of nanoseconds) to large values (microseconds).

Fading distribution, K-factor

The narrow band received signal fading can be characterized by a Ricean fading. The key parameter of this distribution is the K-factor, defined as the ratio of the "fixed" component power and the "scatter" component power. The narrow band K-factor distribution was found to be lognormal, with the median as a simple function of season, antenna height, antenna beamwidth and distance. The model for the K-factor (in linear scale) is as follows:

$$K = F_s F_h F_b K_o d^{\gamma} u \tag{2-10}$$

where

F_s is a season factor; $F_s = 1.0$ in summer; 2.5 in winter

F_h is the received antenna height factor

F_b is the beamwidth factor

K_o and γ are regression coefficients

u is a lognormal variable which has 0 dB mean and a standard deviation of 8 dB.

Using this model, one can observe that the K-factor decreases as the distance increases and as antenna beamwidth increases.

Doppler spectrum

The random components of the coefficients generated in the previous paragraph have a white spectrum since they are independent of each other. The SUI channel model defines a specific power spectral density (PSD) function for these scatter component channel coefficients called “rounded” PSD which is given as

$$S(f) = \begin{cases} 1 - 1.72 f_0^2 + 0.785 f_0^4 & |f_0| \le 1 \\ 0 & |f_0| > 1 \end{cases} \qquad \text{(2-11)}$$

where $f_0 = \dfrac{f}{f_m}$. In fixed wireless channels the shape of the spectrum is therefore different than the classical Jake’s spectrum for mobile channels. Figure 2-18 shows that its shape of Doppler spectrum is convex.

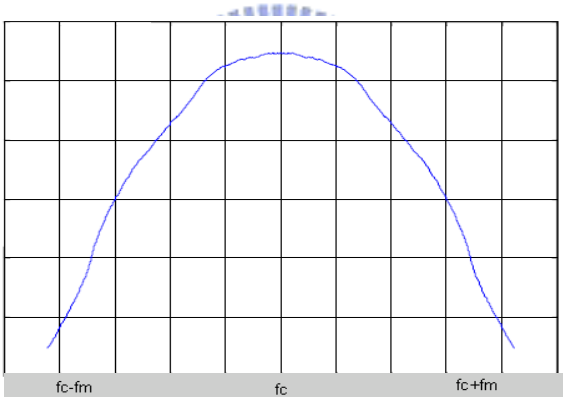

Figure 2-18: Doppler spectrum of SUI channel models

Antenna correlation

The SUI channel models define an antenna correlation, which has to be considered if multiple transmit or receive elements, i.e. multiple channels, are being simulated. Antenna correlation is commonly defined as the envelope correlation coefficient between signals transmitted at two antenna elements. The received baseband signals are modeled as two complex random processes *X(t)* and *Y(t)* with an envelope correlation coefficient of

$$\rho_{env} = \left| \frac{E\left\{ \left(X - E\{X\}\right)\left(Y - E\{Y\}\right)^* \right\}}{\sqrt{E\left\{ \left|X - E\{X\}\right|^2 \right\} E\left\{ \left|Y - E\{Y\}\right|^2 \right\}}} \right|. \quad (2\text{-}12)$$

Note that this is not equal to the correlation of the envelopes of two signals, a measure that is also used frequently in cases where no complex data is available.

Antenna gain reduction factor

The use of directional antennas requires to be considered carefully. The gain due to the directivity can be reduced because of the scattering. The effective gain is less than the actual gain. This factor should be considered in the link budget of a specific receiver antenna configuration.

Denote ΔG_{BW} as the Gain Reduction Factor. This parameter is a random quantity which dB value is Gaussian distributed with a mean μ_{grf} and a standard deviation σ_{grf} given by

$$\mu_{grf} = -(0.53 + 0.1I)\ln(\beta / 360) + (0.5 + 0.04I)(\ln(\beta / 360))^2 \quad (2\text{-}13)$$

$$\sigma_{grf} = -(0.93 + 0.02I)\ln(\beta / 360), \quad (2\text{-}14)$$

where

β is the beamwidth in degrees

I = 1 for winter and I = -1 for summer.

In the link budget computation, if G is the gain of the antenna (dB), the effective gain of the antenna equals $G - \Delta G_{BW}$. For example, if a 20-degree antenna is used, the mean value of ΔG_{BW} would be closed to 7 dB.

2.5 Summary

Specification of IEEE 802.16-2005 system has been introduced in this chapter. We also introduce some key transmit techniques and their operations. By using these transmit techniques, the capacity and range of the system can be improved significantly. Finally, the SUI-3 channel model for slow mobility is introduced.

Chapter 3

Different Cooperative Diversity Schemes for WiMAX Systems

This section describes our analysis based on the following system model in which single antenna terminals are considered and relay stations (RS) are used for relaying in an OFDM wireless network.

3.1 System Model

In broadband communications, OFDM is an effective technique to capture multipath energy, mitigate the intersymbol interference, and offer high spectral efficiency. Therefore, OFDM is used in many communications system including IEEE-802.16 system. Multiple-input-multiple-output (MIMO) signal processing techniques for communication over point-to-point links using multiple collocated antennas at the transmitter and the receiver have improved tremendously in reliability and throughput. These techniques can be employed to improve the weaker link problem. However due to size, cost and hardware in practical issue constraints the use of MIMO techniques, which may not always be feasible and practical especially in small devices. Therefore, the idea of that making single antenna network nodes cooperatively transmit and receive by forming virtual antenna arrays has been proposed recently [5]. This method is broadly named as cooperative communication. In other words, the idea is that users in the network share their information and transmit cooperatively as a virtual antenna array, hence providing diversity without

the requirement of additional antennas at user terminal. Cooperative diversity has recently emerged as a promising alternative to combat fading in wireless channels [6].

Since OFDM is one of the most popular physical-layer technologies for wireless systems and cooperation is a promising architecture for next generation wireless system, the combination of the two techniques named OFDM-relay will be a good candidate technology for future wideband wireless communications. To improve the performance of ODFM based systems, the fundamental concept of cooperative diversity can be employed. However, special cooperation protocols and modulation and coding are needed to efficiently exploit the available multiple carriers. In [15], an oversampling technique is employed to provide efficient resource utilization due to OFDM properties. In [16], an application a space-time cooperation in OFDM systems was proposed.

Here our system model is based on fixed relaying protocols, in which the relays always repeat the source information. Moreover, our studies rely on an assumption of fixed network topology and fixed source-relay pairs. We take IEEE-802.16 system as a reference and consider mobile users with relatively low speed. For these slow mobile users, the channel is almost unchanged for the duration of a frame which consists of a certain number of OFDM symbols. Since users with slow mobility are considered, we use instantaneous SNR as channel state information. Further considerations should be taken for high-mobility users, such as impact of imperfect channel state information, etc.

We consider a time-division transmission in the source-to-relay (S-R), source-to destination (S-D), and relay-to-destination (R-D) links and Time Division Duplexing (TDD) is assumed. Figure 3-1 shows the cooperation system model, where $\gamma_{SD}, \gamma_{SR}, \gamma_{RD}$ are the signal-to noise ratio (SNR) of the S-D link, S-R link, and the R-D link respectively, and σ^2 represents the noise variance. The relay which

is intermediate nodes and present in close vicinity to either the source or destination form the basis for cooperative communication. The cooperative protocol divides the transmission into tow phase. In the first phase, the source transmits its packets to the destination and the packets are also received at the relay due to the broadcast nature. The received signals at destination $y_D[n]$ and relay $y_R[n]$ are

$$y_D[n] = \sqrt{E_s} h_{SD} x[n] + n_D[n], \tag{3-1}$$

and

$$y_R[n] = \sqrt{E_s} h_{SR} x[n] + n_R[n], \tag{3-2}$$

where E_s is the transmit energy at the source, h_{SD} and h_{SR} are the channel coefficients of the S-D link and the S-R link, and $n_D[n]$ and $n_R[n]$ are the noise received at the destination and the relay, respectively. After receiving the source's packet, the relay forwards the signals $\hat{x}[n]$ to the destination at the R-D link, where γ_{RD} represents the SNR of the R-D link. The signals received from the relay at destination $y_D[n+1]$ is

$$y_D[n+1] = \sqrt{E_R} h_{RD} \hat{x}[n] + n_D[n+1], \tag{3-3}$$

where E_R is the transmit energy at the relay, and h_{RD} is the channel coefficients of the R-D link. After receiving the signals during two phases, the destination combines two signals from the source and the relay to make decision. Next we study the basic relaying models based on the cooperative communication system studied.

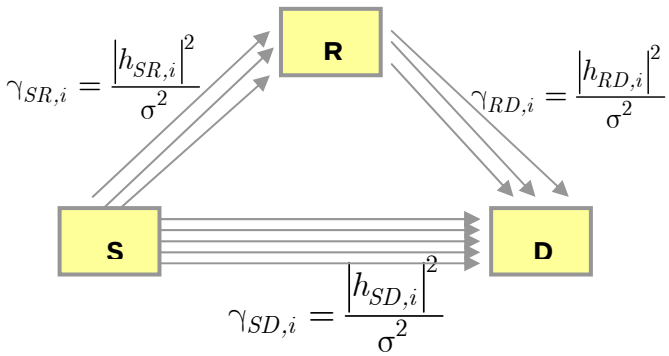

Figure 3-1: Illustration of Cooperative transmission

3.1.1 Relaying methods

Two basic relaying methods are commonly used for cooperation [17].

Decode and forward:

In decode and forward method, the relay first decodes signals received from the source, re-encodes the signals, and then retransmits them. The receiver at the destination uses information retransmitted from the relay and the source to make decisions. It should be noted that it is possible for the relay to decode symbols in error resulting in error propagation. Perfect regeneration at the relays may require retransmission of symbols or use of forward error correction (FEC) depending on the quality of the channel between the source and the relay. This may not be suitable for a delay limited networks.

Amplify and forward:

In this method each cooperating node receives the signals transmitted by the source node but do not decode them. These signals in noisy form are amplified to compensate for the attenuation suffered between the S-R link and retransmitted. The destination requires knowledge of the channel state between the S-R link to correctly decode the symbols sent from the source. This requires transmission of pilots over the relays resulting in overhead in terms of additional bandwidth. Additionally sampling, amplifying, and retransmitting analog values is a nontrivial task for real-time implementation.

3.2 Different Cooperative Diversity Schemes

This section describes various cooperative schemes: cooperative-multiple input single output (MISO) and cooperative-single input multiple output (SIMO) are considered to achieve diversity. Trying various cooperative diversity schemes for

OFDM and OFDMA TDD based networks (802.16e) in low mobility scenarios to maximize system end-to-end throughput. The average transmit energy of the source and relay terminals per sub-carrier is fixed and represented by E_s and E_R, respectively.

3.2.1 Cooperative Receive Diversity Scheme

In the first time slot of cooperative receive diversity scheme, the source transmits the signals while both the relay and the destination receive and both the relay and the destination bugger this information. In the second time slot, the relay forwards the signals to destination and the BS remains silent. For each one of the AF or DF based forwarding, the destination combines the signals received form the source and the destination via Maximum Ratio Combining (MRC) [18]. After MRC, the destination achieves cooperative receive diversity. We refer it to Cooperative-single input multiple output scheme (Coop-SIMO), as shown in Figure 3-2. The derivations are done for a given sub-carrier. In the following sub-sections, the equivalent end-to-end instantaneous SNR is derived for both AF and DF based relaying.

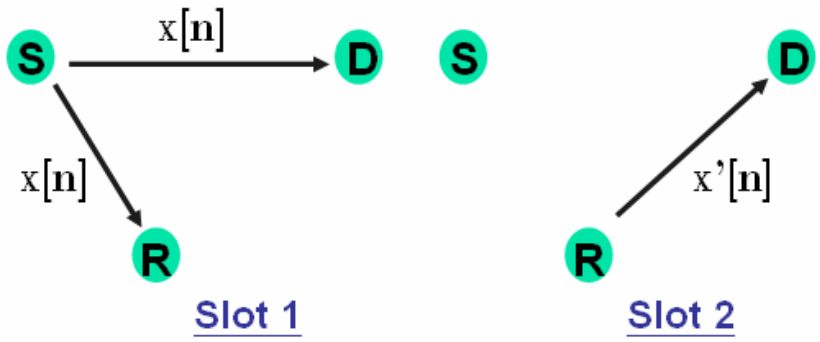

Figure 3-2: Coop-SIMO diversity scheme

- **AF Based Coop-SIMO Diversity Scheme**

In the AF mode, the relay terminal amplifies and forwards the signal received

from the source. The transmitted signal by the relay using AF at sub-carrier i is given by

$$S_R^{AF}[n+1] = \frac{\sqrt{E_R}}{\beta} y_R[n], \tag{3-4}$$

where $\beta = \sqrt{N_o(1+\gamma_{SR})}$ is adapted such that $E_R = E\left\{\left|s_R^{AF}[n+1]\right|^2\right\}$, and $y_R[n]$ is the signal which received from the S-R link.

The received baseband signal at the destination at sub-carrier i over two successive OFDM symbols can be written as

$$\begin{aligned} Y_{SIMO}^{AF} &= \begin{bmatrix} y_D[n] \\ y_D[n+1]^{AF} \end{bmatrix} = \begin{bmatrix} h_{SD}\sqrt{E_S}x[n] + n_D[n] \\ h_{RD}\dfrac{\sqrt{E_R}}{\beta} y_R[n] + n_D[n+1] \end{bmatrix} \\ &= \begin{bmatrix} h_{SD}\sqrt{E_S}x[n] + n_D[n] \\ \dfrac{\sqrt{E_S}\sqrt{E_R}}{\beta} h_{SR}h_{RD}x[n] + \dfrac{\sqrt{E_R}}{\beta} h_{RD}n_R[n] + n_D[n+1] \end{bmatrix} \\ &= \begin{bmatrix} \sqrt{E_S}h_{SD} \\ \dfrac{\sqrt{E_R}\sqrt{E_S}}{\beta} h_{SR}h_{RD} \end{bmatrix} x[n] + \begin{bmatrix} n_D[n] \\ \dfrac{\sqrt{E_R}}{\beta} h_{RD}n_R[n] + n_D[n+1] \end{bmatrix} \\ &= \mathrm{H}_{SIMO}^{AF} x[n] + \mathrm{n}_{SIMO}^{AF}, \end{aligned} \tag{3-5}$$

where H_{SIMO}^{AF} and n_{SIMO}^{AF} are given by

$$\mathrm{H}_{SIMO}^{AF} = \begin{bmatrix} h_{SD}\sqrt{E_S} \\ \dfrac{\sqrt{E_S}\sqrt{E_R}}{\beta} h_{SR}h_{RD} \end{bmatrix}, \tag{3-6}$$

$$\mathrm{n}_{SIMO}^{AF} = \begin{bmatrix} n_D[n] \\ \dfrac{\sqrt{E_R}}{\beta} h_{RD}n_R[n] + n_D[n+1] \end{bmatrix}, \tag{3-7}$$

and $y_D[n]$ is the signal received from the source at the time slot 1 and $y_D^{AF}[n+1]$ is the signal forwarded by the relay based on AF mode.

Assuming that the destination has perfect channel state information (CSI), which are the channel coefficients h_{SD}, h_{SR}, and h_{RD}. We combine the received signals from the source and the relay by MRC:

$$\begin{aligned} z_{SIMO}^{AF} &= \left(\mathrm{H}_{SIMO}^{AF}\right)^{H} Y_{SIMO}^{AF} \\ &= \left(\mathrm{H}_{SIMO}^{AF}\right)^{H} \mathrm{H}_{SIMO}^{AF} x[n] + \left(\mathrm{H}_{SIMO}^{AF}\right)^{H} \mathrm{n}_{SIMO}^{AF}. \end{aligned} \tag{3-8}$$

The instantaneous SNR per symbol achieved after MRC in the AF mode can be derived form (3-8) as follows:

$$\gamma_{SIMO}^{AF} = \frac{\left(\gamma_{SD} + \frac{\gamma_{SR}\gamma_{RD}}{1+\gamma_{SR}}\right)^{2}}{\gamma_{SD} + \frac{\gamma_{SR}\gamma_{RD}}{1+\gamma_{SR}} + \frac{\gamma_{SR}\gamma_{RD}^{2}}{\left(1+\gamma_{SR}\right)^{2}}}. \tag{3-9}$$

After combining the signals at the sub-carrier i, the destination observes a post processing SNR as given by (3-9), which can be referred as that of an effective end-to-end link. In an end-to-end flat fading link with instantaneous SNR γ, the end-to-end throughput can be given as

$$thr(\gamma) = R(\gamma)\big(1 - PER(\gamma)\big), \tag{3-10}$$

where the term $R(\gamma)$ in $b/s/Hz$ represents the nominal rate of the specific modulation and coding and the term $PER(\gamma)$ represents the packet error rate with the specific modulation and coding based on SNR γ [19]. With AF based relaying at the sub-carrier i, the end-to-end throughput based on cooperative receive diversity scheme is finally given by

$$\rho_{SIMO}^{AF} = \frac{1}{2} thr\left(\gamma_{SIMO}^{AF}\right), \tag{3-11}$$

where the factor of 0.5 accounts for the fact that two times of time slots is needed for cooperative transmission compared to direct transmission.

- **DF Based Coop-SIMO Diversity Scheme**

When the relay uses the DF mode at a given sub-carrier, it detects and decodes the signal received from the S-R link at the given sub-carrier. Then, the relay encodes and then forwards it to the destination. Let $\hat{x}[n]$ represent the decoded decision with unit energy. The decision of the relay severely affects the performance of the DF mode. If the relay decodes $x[n]$ incorrectly, it causes the error propagation.

In the DF mode, the relay terminal decodes and forwards the signal received from the source. In the first time slot, the relay demodulates the OFDM symbols received from the source. After the FFT operation, the relay decodes the signal at each sub-carrier and performs cyclic redundancy check (CRC) to check the packets that are correctly received. The relay only encodes and forwards the packets that are correctly received. At the end of the first time slot, it informs the destination about the decoding status of each packet. The transmitted signal by the relay using DF at sub-carrier i is given by

$$s_R^{DF}[n+1] = \sqrt{E_R}\,\hat{x}[n]. \tag{3-12}$$

The received baseband signal at the destination at sub-carrier i over two successive OFDM symbols can be written as

$$\begin{aligned} Y_{SIMO}^{DF} &= \begin{bmatrix} y_D[n] \\ y_D[n+1]^{DF} \end{bmatrix} = \begin{bmatrix} h_{SD}\sqrt{E_S}\,x[n] + n_D[n] \\ h_{RD}\sqrt{E_R}\,\hat{x}[n] + n_D[n+1] \end{bmatrix} \\ &= \begin{bmatrix} \sqrt{E_S}h_{SD} \\ \sqrt{E_R}h_{RD} \end{bmatrix} x[n] + \begin{bmatrix} n_D[n] \\ n_D[n+1] \end{bmatrix} \\ &= \mathrm{H}_{SIMO}^{DF} x[n] + \mathrm{n}_{SIMO}^{DF}, \end{aligned} \tag{3-13}$$

where H_{SIMO}^{DF} is given by

$$\mathrm{H}_{SIMO}^{DF} = \begin{bmatrix} \sqrt{E_S}h_{SD} \\ \sqrt{E_R}h_{RD} \end{bmatrix}, \tag{3-14}$$

and n_{SIMO}^{DF} is given by

$$\mathrm{n}_{SIMO}^{DF} = \begin{bmatrix} n_D[n] \\ n_D[n+1] \end{bmatrix}. \tag{3-15}$$

Assuming that the destination has perfect channel state information (CSI), which the channel coefficients are h_{SD} , h_{SR} , and h_{RD}. We combine the received signals from the source and the relay by MRC:

$$z_{SIMO}^{DF} = \left(\mathrm{H}_{SIMO}^{DF}\right)^{H} \mathrm{Y}_{SIMO}^{DF}. \tag{3-16}$$

Since the relay only forwards when it can decode the packets correctly, the post processing instantaneous SNR achieved at the destination can be derived from (3-16):

$$\gamma_{SIMO}^{DF} = \frac{\left\|\mathrm{H}_{SIMO}^{DF}\right\|_F^2}{N_o^D} = \gamma_{SD} + \gamma_{RD} \tag{3-17}$$

The available data rate of multi-hop is determined by the link with minimal capacity. Therefore, the end-to-end throughput with DF based relaying is the minimum of the end-to-end throughout of the S-R link and the effective R-D and S-D link, respectively. On the other hand, if $\gamma_{SIMO}^{DF} > \gamma_{SR}$, the end-to-end throughput is determined by γ_{SR} ; if $\gamma_{SIMO}^{DF} < \gamma_{SR}$, the end-to-end throughput is determined by γ_{SIMO}^{DF}. Therefore, With DF based relaying at the sub-carrier i, the end-to-end throughput based on cooperative receive diversity scheme is finally given by

$$\rho_{SIMO}^{DF} = \begin{cases} \frac{1}{2} thr\left(\gamma_{SIMO}^{DF}\right) P_c\left(\gamma_{SR}\right) & \gamma_{SIMO}^{DF} < \gamma_{SR} \\ \frac{1}{2} thr\left(\gamma_{SR}\right) P_c\left(\gamma_{SIMO}^{DF}\right) & \gamma_{SIMO}^{DF} > \gamma_{SR} \end{cases}, \tag{3-18}$$

where $P_c(\gamma)$ represents the probability of correct reception of a packet based on SNR γ and the factor of 0.5 accounts for the fact that two times of time slots is needed for cooperative transmission compared to direct transmission.

3.2.2 Cooperative Transmit Diversity Scheme

In order to achieve cooperative transmit diversity, in the first time slot, only the relay listens to the broadcast of the source. In the second time slot, both the source and the relay transmit simultaneously by using the same radio resource. This way, an equivalent MISO channel is observed at the destination by cooperative transmission. Therefore, the cooperative transmit diversity scheme can be refereed to as Cooperative-multiple input single output scheme (Coop-MISO), as shown in Figure 3-3.

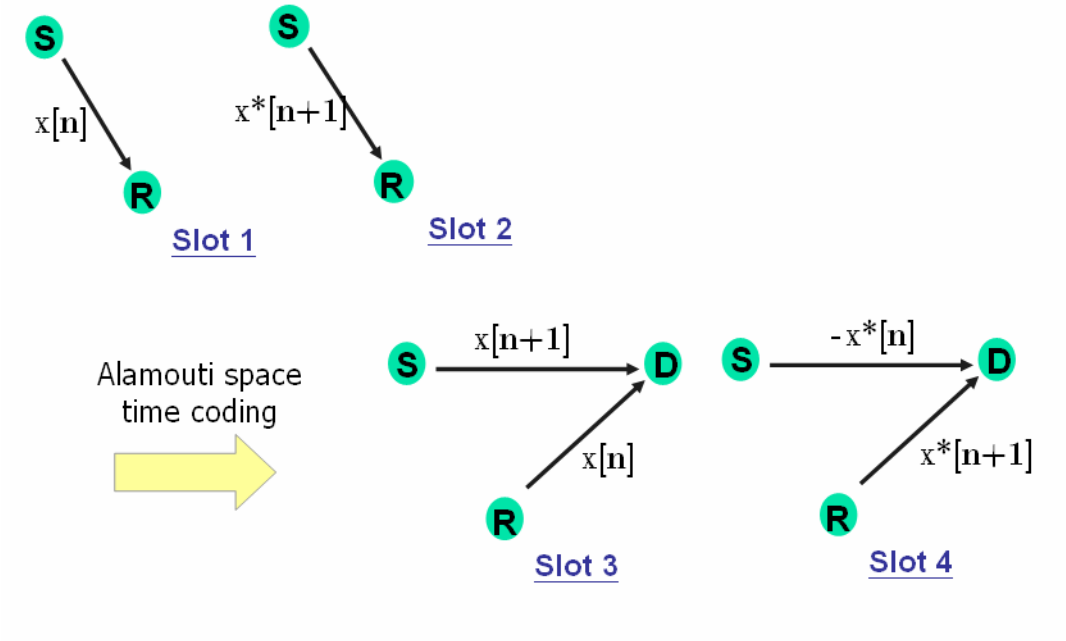

Figure 3-3: Coop-MISO diversity scheme

To achieve diversity, cooperative space time coding is used by the source and the relay [20] and we employ Alamouti spce time coding [21]. When Coop-MISO scheme is employed, the time slot is divided into four sub time slots. During the first tow time slots, the relay listens to the source only; During the second two time slots, both the relay and the source transmit simultaneously employing Alamouti space-time coding. The time division transmission structure to achieve cooperative transmit diversity with Alamouti space-time coding is presented in Table 1. In the table, S represents the

source and R represents the relay and D represents the destination, respectively. The derivations are done for a given sub-carrier. In the following sub-sections, the equivalent end-to-end instantaneous SNR is derived for both AF and DF based relaying. The transmission sequence presented in Table 3-1 has bean considered.

Table 3-1: Transmission sequence of Coop-MISO scheme

First phase	First phase	Second phase	Second phase
nth symbol	n+1st symbol	N+2nd symbol	N+3nd symbol
S→R : $x[n]$	S→R : $-x^*[n+1]$	S→D : $x[n+1]$	S→D : $x^*[n]$
		R→D : $x[n]$	R→D : $-x^*[n+1]$

- **AF Based Coop-MISO Diversity Scheme**

In the AF mode, the relay terminal amplifies and forwards the signal received from the source. In the first phase, the relay amplifies the signal at each sub-carrier and buffers for the cooperative transmission in the second phase. During the second phase, the transmitted signal by the relay using AF at sub-carrier i is given by

$$S_R^{AF}[n+2] = \frac{\sqrt{E_R}}{\beta} y_R[n] = \frac{\sqrt{E_R}}{\beta} h_{SR} x[n] + \frac{\sqrt{E_R}}{\beta} n_R[n], \tag{3-19}$$

and

$$\begin{aligned} S_R^{AF}[n+3] &= \frac{\sqrt{E_R}}{\beta} y_R[n+1] \\ &= -\frac{\sqrt{E_R}}{\beta} h_{SR} x^*[n+1] + \frac{\sqrt{E_R}}{\beta} n_R[n+1], \end{aligned} \tag{3-20}$$

where $\beta = \sqrt{N_o(1+\gamma_{SR})}$ is adapted such that $E_R = E\left\{\left|s_R^{AF}[n+1]\right|^2\right\}$, and $y_R[n]$, and $y_R[n+1]$ are the signals which received from the S-R link during the first phase.

At the end of the tow phases at a given sub-carrier i, the received baseband signal at the destination over two successive OFDM symbols can be written as

$$
\begin{aligned}
Y_{MISO}^{AF} &= \begin{bmatrix} y_D[n+2] \\ y_D[n+3] \end{bmatrix} \\
&= \begin{bmatrix} h_{SD}x[n+1] + h_{RD}s_{MISO}^{AF}[n+2] + n[n+2] \\ h_{SD}x^*[n] + h_{RD}s_{MISO}^{AF}[n+3] + n[n+3] \end{bmatrix} \\
&= \begin{bmatrix} \frac{\sqrt{E_R E_S}}{\beta} h_{SR}h_{RD} & \sqrt{E_S}h_{SD} \\ \sqrt{E_S}h_{SD}^* & -\frac{\sqrt{E_R E_S}}{\beta} h_{SR}^* h_{RD}^* \end{bmatrix} \begin{bmatrix} x_i[n] \\ x_i[n+1] \end{bmatrix} \\
&\quad + \begin{bmatrix} n_D[n+2] + h_{RD}\frac{\sqrt{E_R}}{\beta} n_R[n] \\ \left(n_D[n+3] + h_{RD}\frac{\sqrt{E_R}}{\beta} n_R[n+1] \right)^* \end{bmatrix} \\
&= \begin{bmatrix} h_1 & h_2 \\ h_2^* & -h_1^* \end{bmatrix} \begin{bmatrix} x_i[n] \\ x_i[n+1] \end{bmatrix} + \begin{bmatrix} n_1 \\ n_2^* \end{bmatrix} \\
&= \mathrm{H}_{eff}\mathrm{x} + \mathrm{n},
\end{aligned}
\tag{3-21}
$$

where $h_1 = \frac{\sqrt{E_R E_S}}{\beta} h_{SR}h_{RD}$ and $h_2 = \sqrt{E_S}h_{SD}$. The noise components n_j where $j \in \{1,2\}$ is given by

$$
n_1 = n_D[n+2] + h_{RD}\frac{\sqrt{E_R}}{\beta} n_R[n], \tag{3-22}
$$

and

$$
n_2 = n_D[n+3] + h_{RD}\frac{\sqrt{E_R}}{\beta} n_R[n+1]. \tag{3-23}
$$

At the end of two phases, the 1×2 cooperative-MISO channel H_{MISO}^{AF} achieved with AF based relaying is given by

$$
\mathrm{H}_{MISO}^{AF} = \begin{bmatrix} h_1 & h_2 \end{bmatrix} = \begin{bmatrix} \frac{\sqrt{E_S}\sqrt{E_R}}{\beta} h_{SR}h_{RD} & \sqrt{E_S}h_{SD} \end{bmatrix}. \tag{3-24}
$$

Assuming that the destination has perfect channel state information (CSI), which

the channel coefficients are h_{SD}, h_{SR},and h_{RD}. We combine the received signals from the source and the relay by MRC:

$$z_{MISO}^{AF} = \left(\mathrm{H}_{eff}\right)^{\mathrm{H}} \mathrm{y}_{MISO}^{AF} = \begin{bmatrix} h_1^{*} & h_2 \\ h_2^{*} & -h_1 \end{bmatrix} \left(\begin{bmatrix} h_1 & h_2 \\ h_2^{*} & -h_1^{*} \end{bmatrix} \mathrm{x} + \mathrm{n} \right)$$

$$= \begin{bmatrix} |h_1|^2 + |h_2|^2 & 0 \\ 0 & |h_1|^2 + |h_2|^2 \end{bmatrix} \mathrm{x} + \begin{bmatrix} h_1^{*} & h_2 \\ h_2^{*} & -h_1 \end{bmatrix} \mathrm{n}$$

$$= \left\| \mathrm{H}_{MISO}^{AF} \right\|_F^2 \mathrm{x} + \tilde{\mathrm{n}} \,, \tag{3-25}$$

where

$$\tilde{\mathrm{n}} = \begin{bmatrix} \widetilde{n_1} \\ \widetilde{n_2} \end{bmatrix} = \left(\mathrm{H}_{eff}\right)^{\mathrm{H}} \mathrm{n} = \begin{bmatrix} h_1^{*} n_1 + h_2 n_2^{*} \\ h_2^{*} n_1 - h_1 n_2^{*} \end{bmatrix}. \tag{3-26}$$

The instantaneous SNR per symbol achieved after MRC in the AF mode can be derived form (3-24) as follows:

$$\gamma_{MISO}^{AF} = \frac{\left(\left\| \mathrm{H}_{MISO}^{AF} \right\|_F^2 \right)^2}{\mathrm{E}\left\{ \left| \widetilde{n_1} \right|^2 \right\}} = \gamma_{SD} + \frac{\gamma_{SR}\gamma_{RD}}{1 + \gamma_{SR} + \gamma_{RD}}. \tag{3-27}$$

Therefore, with AF based relaying at the sub-carrier i, the end-to-end throughput based on cooperative transmit diversity scheme is finally given by

$$\rho_{MISO}^{AF} = \frac{1}{2} thr\left(\gamma_{MISO}^{AF}\right), \tag{3-28}$$

where the factor of 0.5 accounts for the fact that two times of time slots is needed for cooperative transmission compared to direct transmission.

- **Coop-MISO Diversity Schemes with DF based**

When the relay uses the DF mode at a given sub-carrier, it detects and decodes the signal received from the S-R link at the given sub-carrier. Then, the relay encodes and forwards it to the destination. In the first phase, the relay demodulates the OFDM symbols received from the source. After the FFT operation, the relay decodes the

signal at each sub-carrier. In the second phase, the relay and the source make cooperative transmission using space time block codes. Unlike Coop-SIMO diversity scheme, the relay only re-encoder and buffers the packets that are correctly received. At the end of the first phase, the relay informs the source and the destination about the decoding status of each packet. The transmitted signal by the relay using DF at sub-carrier i is given by

$$\begin{aligned} s_R^{DF}[n+2] &= \sqrt{E_R}\,\hat{x}[n] \\ s_R^{DF}[n+3] &= \sqrt{E_R}\,\hat{x}[n+1] \end{aligned} \tag{3-29}$$

Since the relay buffers only when it can decode the packets which are correctly received, the post processing instantaneous SNR achieved at the destination after Alamouti scheme based space-time decoding can be derived as [18], [21]:

$$\gamma_{MISO}^{DF} = \frac{\left\| \mathrm{h}_{MISO}^{DF} \right\|_F^2}{N_o} = \gamma_{SD} + \gamma_{RD}\,, \tag{3-30}$$

where h_{MISO}^{DF} is

$$\mathrm{h}_{MISO}^{DF} = \begin{bmatrix} \sqrt{E_S} h_{SD} \\ \sqrt{E_R} h_{RD} \end{bmatrix}. \tag{3-31}$$

Similar to Coop-SIMO, with DF based relaying at the sub-carrier i, the end-to-end throughput based on cooperative transmit diversity scheme is finally given by

$$\rho_{MISO}^{DF} = \begin{cases} \frac{1}{2} thr\left(\gamma_{MISO}^{DF}\right) P_c\left(\gamma_{SR}\right) & \gamma_{MISO}^{DF} < \gamma_{SR} \\ \frac{1}{2} thr\left(\gamma_{SR}\right) P_c\left(\gamma_{MISO}^{DF}\right) & \gamma_{MISO}^{DF} > \gamma_{SR}. \end{cases} \tag{3-32}$$

3.3 Evaluation of Overall Average BER Upper Bound Based on AF Mode

In many wireless communication systems, convolution codes are employed to improve performance, such as 802.11, 802.16 (WiMAX), etc. In this section, the overall average BER based on AF mode is evaluated according to the equivalent post processing instantaneous SNR we derived early.

We begin this section by analyzing the performance bounds for convolutional codes. According to coding theorem [22] [23], in general, assuming the incorrect path has weight d, a first event error is made with probability

$$P_d(\gamma) = \begin{cases} \sum_{e=d+1/2}^{d} \binom{d}{e} p^e(\gamma)\left(1-p(\gamma)\right)^{d-e} \\ \frac{1}{2}\binom{d}{d/2} p^{\frac{d}{2}}(\gamma)\left(1-p(\gamma)\right)^{\frac{d}{2}} + \sum_{e=d/2+1}^{d} \binom{d}{e} p^e(\gamma)\left(1-p(\gamma)\right)^{d-e} \end{cases}, \quad (3\text{-}33)$$

where $p(\gamma) = Q\left(\sqrt{\gamma}\right)$ is the BER under SNR γ without coding. Because all incorrect paths can cause a first event error, the event error probability can be bounded, using a union bound, by the sum of the error probability of those incorrect paths. Therefore, the event error probability of convolution code $P_e(\gamma)$ can be bounded by

$$P_e(\gamma) < \sum_{d=d_{free}}^{\infty} A_d P_d(\gamma), \quad (3\text{-}34)$$

where A_d is the number of codewords of weight d.

The bound of (3-33) can be further simplified by noting that for *d* odd,

$$
\begin{aligned}
P_d(\gamma) &= \sum_{e=d+1/2}^{d} \binom{d}{e} p^e(\gamma)\big(1-p(\gamma)\big)^{d-e} \\
&< \sum_{e=d+1/2}^{d} \binom{d}{e} p^{\frac{d}{2}}(\gamma)\big(1-p(\gamma)\big)^{\frac{d}{2}} \\
&= p^{\frac{d}{2}}(\gamma)\big(1-p(\gamma)\big)^{\frac{d}{2}} \sum_{e=d+1/2}^{d} \binom{d}{e} p \\
&< \sum_{e=0}^{d} \binom{d}{e} p^{\frac{d}{2}}(\gamma)\big(1-p(\gamma)\big)^{\frac{d}{2}} \\
&= 2^d p^{\frac{d}{2}}(\gamma)\big(1-p(\gamma)\big)^{\frac{d}{2}} \ . \qquad \text{(3-35)}
\end{aligned}
$$

It can also be shown that (3-35) is an upper bound on $P_d(\gamma)$ for d even. Hence, the bound of (3-35) can be applied to (3-34), the event error probability of convolution code $P_e(\gamma)$ can be bounded by

$$
P_e(\gamma) < \sum_{d=d_{free}}^{\infty} A_d P_d(\gamma) < \sum_{d=d_{free}}^{\infty} A_d \left[2\sqrt{p(\gamma)\big(1-p(\gamma)\big)}\right]^d . \qquad \text{(3-36)}
$$

For small $p(\gamma)$, the bound is dominated by its first term which is the free distance term, and the event error probability of convolution code $P_e(\gamma)$ can be approximated as

$$
P_e(\gamma) \approx A_{d_{free}} \left[2\sqrt{p(\gamma)\big(1-p(\gamma)\big)}\right]^{d_{free}} \approx A_{d_{free}} 2^{d_{free}} p(\gamma)^{\frac{d_{free}}{2}} . \qquad \text{(3-37)}
$$

The error event probability bound of (3-37) can be modified to provide a bound on the bit error probability $P_b(\gamma)$. Each event error causes a number of information bit errors equal to the number of nonzero information bits on the incorrect path. Therefore, if each error event probability term $P_e(\gamma)$ is weighted by the number of nonzero information bits on the weight d path, the bound can be divided by k, the number of information per unit time, to obtain a bound on $P_b(\gamma)$. In other words, according to the deviation of the error event probability, the bit error probability is

bounded by

$$\begin{aligned} P_e(\gamma) &< \sum_{d=d_{free}}^{\infty} B_d P_d(\gamma) \\ &< \sum_{d=d_{free}}^{\infty} B_d \left[2\sqrt{p(\gamma)(1-p(\gamma))}\right]^d \\ &\approx B_{d_{free}} \left[2\sqrt{p(\gamma)(1-p(\gamma))}\right]^{d_{free}} \\ &\approx B_{d_{free}} 2^{d_{free}} p(\gamma)^{\frac{d_{free}}{2}} , \end{aligned} \tag{3-38}$$

where B_d is the total number of nonzero information bits on all weight-d paths, divided by the number of information bits k per unit time.

Here we assume the encoder and decoder diagram is [2,1,3] , we can derive the WEF (codeword weight enumerating function) $A(x)$ as

$$\begin{aligned} A(X) &= \frac{X^{12} + X^7(1-X) + X^{11}(1-X) + X^6\left(1-2X+X^2\right) + X^8 + X^7(1-X) + X^7\left(1-X-X^4\right)}{1-2X-X^3} \\ &= \frac{X^6 + X^7 - X^8}{1-2X-X^3} \\ &= X^6 + 3X^7 + 5X^8 + 11X^9 + 25X^{10} + \cdots, \end{aligned} \tag{3-39}$$

and the bit WEF $B(x)$ can be calculated directly form the codeword WEF $A(w,x)$ as

$$\begin{aligned} B(X) &= \sum_d B_d X^d = \frac{1}{k}\frac{\partial A(W,X)}{\partial W}\bigg|_{W=1} \\ &= \frac{\partial\left[W^2X^6 + \left(W+2W^3\right)X^7 + \left(W^2+4W^4\right)X^8 + \cdots\right]}{\partial W}\bigg|_{W=1} \\ &= 2X^6 + 7X^7 + 18X^8 + \cdots . \end{aligned} \tag{3-40}$$

According to the instantaneous SNR per symbol achieved after MRC in the AF mode of Coop-MISO and Coop-SIMO we derived above, we can achieve BER upper bound for Coop-MISO scheme by substituting γ_{AF}^{MISO} for γ in (3-38) and BER upper bound for Coop-SIMO scheme by substituting γ_{AF}^{SIMO} for γ in (3-38).

3.4 Implementing Cooperative Transmission in WiMAX Systems

In this section, we design a cooperative system based on OFDM. In order to implement different cooperative diversity schemes in WiMAX systems, our design is to modify the IEEE 802.16 OFDM and IEEE 802.16e OFDMA system for cooperative transmission, including most of the physical layer components, including the transmitter and receiver architecture and the frame structure. The cooperative transmission is based on a two-phase transmission of each frame. The performance of the cooperative-OFDM system with different cooperative diversity schemes mentioned before is extensively evaluated through simulations. We consider a communication scenario where only one relay node helps the source relay information data to the destination. Each node is assumed to transmit or receive signals with only on antenna at the same frequency.

Figure 3-4 illustrates a block diagram of the Coop-SIMO OFDM based system transmitter and receiver for WiMAX systems. The structure of the transmitter is similar to that of the IEEE 802.16 standard [1]. Data bits are first scrambled by a side-stream scrambler with four different seed values as in [2], and they are encoded using a RS-CC encoder. Encoded bits are interleaved by an $n_{row} \times n_{col}$ block interleaver and then modulated into transmit symbols by a given modulation scheme. A series of N_d symbols are loaded on OFDM data sub-carriers, and N_p pilot symbols and Ng guard or null symbols are loaded on corresponding sub-carriers. Thus, the total number of sub-carriers is $N = N_d + N_p + N_g$=256 among which $N_u = N_d + N_p$ =192 sub-carriers are dedicated to data or pilots. An inverse fast Fourier transform (IFFT) of the N symbols results in N samples of time domain signals. A cyclic prefix

of L_{cp} samples is appended in front of the N time domain samples to form a complete OFDM symbol. Here we take L_{cp} =1/16 N. To implement transmit windowing, additional cyclic prefix and postfix samples are then attached. For simplicity of our simulations, we ignore transmit windowing here, since it does not affect the error performance when the delay spread and the timing error are less than the length of cyclic prefix. Correspondingly, each OFDM symbol consists of $L_{sym} = N + L_{cp} = 320$ samples. The receiver first establishes timing and frequency synchronization and then estimates channel responses using the received preamble signals after FFT. Second, each OFDM symbol is demodulated according to the inverse procedure of the transmitter. In particular, the soft-decision Viterbi algorithm [23] is employed to decode the convolutional encoded data bits.

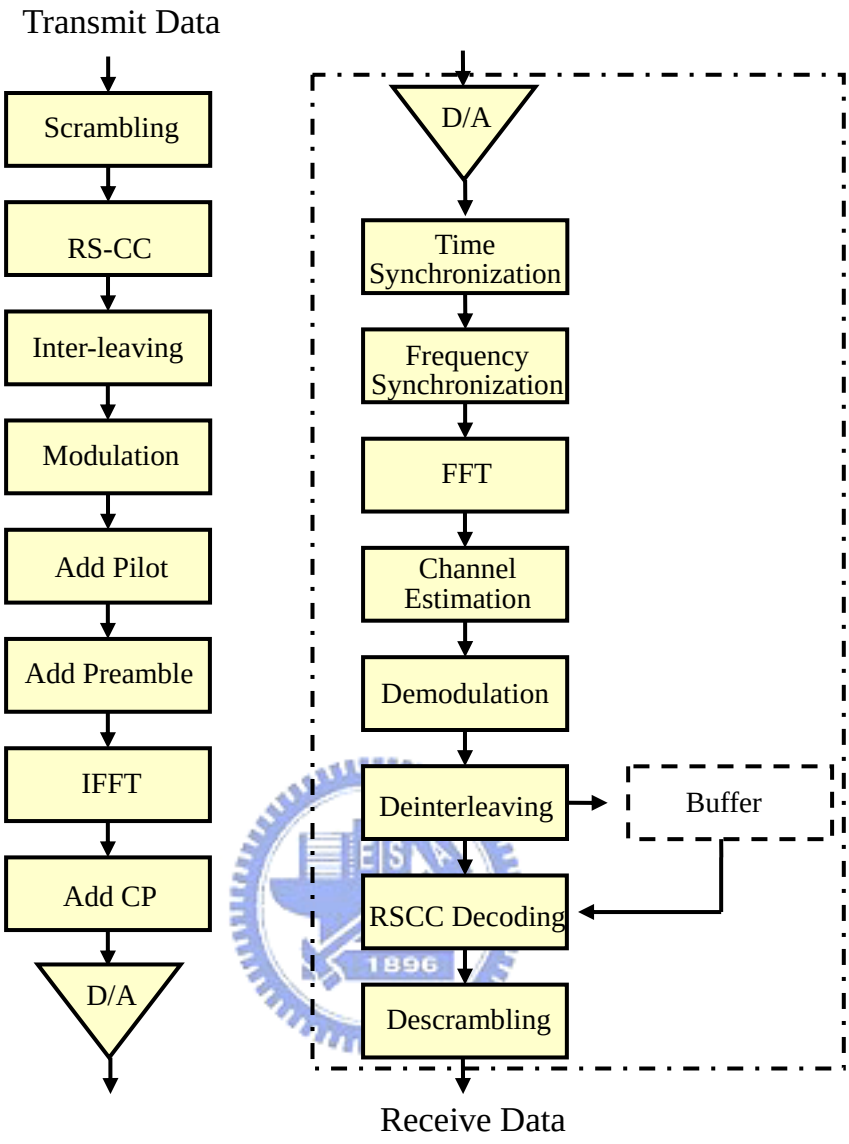

Figure 3-4: Block diagram of the Coop-SIMO OFDM based system

First, the main difference between traditional OFDM based receiver and Coop-SIMO OFDM-based receiver is that Coop-SIMO receiver includes an additional buffer for data of time slot 1 before Viterbi decoder. The buffer is needed for saving the data of time slot 1 received from the source. Because Coop-SIMO can be viewed as virtual SIMO system, the Viterbi decoder should do the decoding process according to the data of time slot 1 received from the source and the data of time slot 2 received from the relay. Second, due to channel estimation error, we

multiply the weighting coefficients to the bits of each time slot before combining, as Figure 3-5 shows. Channel estimation error is proportional to the instantaneous SNR conditions; in other words, when instantaneous SNR at the receiver is higher, the result of channel estimation will be more accurate. Furthermore, the accuracy of channel estimation affects the correctness of Viterbi decoding. Therefore, instantaneous SNR conditions influence the performance of decoding.

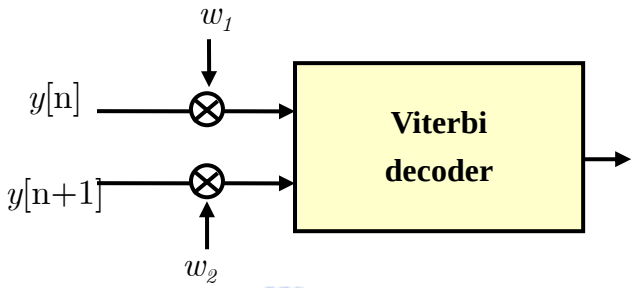

Figure 3-5: Block diagram of weighting algorithm

Here we received data of two time slots; the instantaneous SNR of the data received at time slot 1 is according to direct link h_{SD} and instantaneous SNR of the data received at time slot 2 is according to relay channel h_{SR} and h_{RD}. Because the instantaneous SNR of two time slots is affected by different channel respectively, the accuracy of decoding is also different. Therefore, the weighting coefficients multiplied before combining are proportional to channel conditions of each time slots. The weighting coefficients of time slot 1 w_1 and the weighting coefficients of time slot 2 w_2 are given by:

$$w_1 = \frac{\gamma_{SR}}{\gamma_{SR} + \gamma_{relay}}$$
$$w_2 = \frac{\gamma_{relay}}{\gamma_{SR} + \gamma_{relay}}, \quad (3\text{-}41)$$

where γ_{relay} is the equivalent instantaneous SNR of the S-R link and R-D link.

For AF based relaying, $\gamma_{relay} = \gamma^{AF}$. For DF based relaying, $\gamma_{relay} = \gamma_{RD}$.

Figure 3-6 illustrates the block diagram of the Coop-MISO OFDM based system transmitter and receiver for WiMAX systems. The structure is similar to Coop-SIMO receiver. The only difference between Coop-MISO receiver and Coop-SIMO receiver is that the additional buffer is no need for Coop-MISO receiver. Because Coop-MISO can be refer as to virtual MISO system as mentioned before, the structure of Coop-MISO system is the same as the traditional MISO system. In other words, the relay here can be viewed as an antenna of the base station to build a MISO system, so the advantage of Coop-MISO system is that the structure of Coop-MISO system is almost the same as the traditional MISO system. It is more practical for employing the cooperative diversity in WiMAX systems.

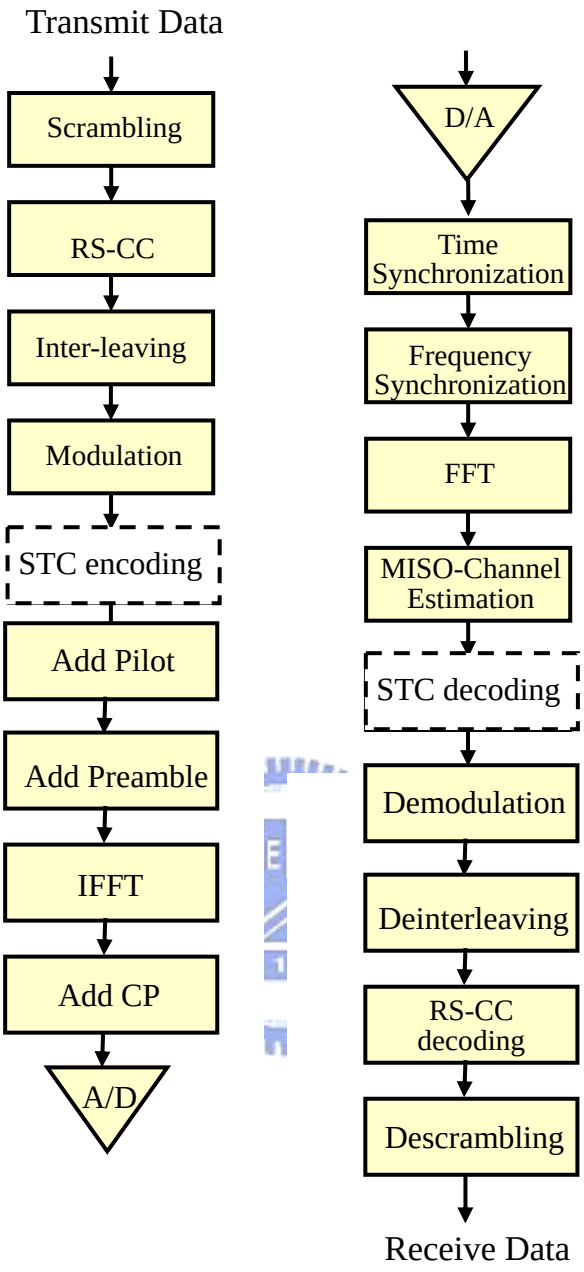

Figure 3-6: Block diagram of the Coop-SIMO OFDM based system

3.5 Computer Simulations

In this section, computer simulation results are conducted to verify the upper bounds of each cooperative diversity scheme we derived in Section 3-3. In the following simulations, the channel is slow Rayleigh fading channel with AWGN. We use convolutional code with generator [2,1,3] and QPSK modulation. Figure 3-7 plots

the analytical bound and simulation results of BER as a function of the transmit SNR. Investigating the BER at high SNR region and comparing with the analytical bounds, it is clear that two cooperative diversity schemes can both achieve diversity as we expected. The figure shows that the analytical bounds are close to the simulations both in Coop-MISO and Coop-SIMO cooperative diversity schemes. Furthermore, comparing two cooperative diversity schemes, Coop-SIMO can achieve nearly 2 dB gain over Coop-MISO. Because Coop-SIMO can be referred as to a virtual SIMO system, it can gain additional antenna gain comparing with MISO system.

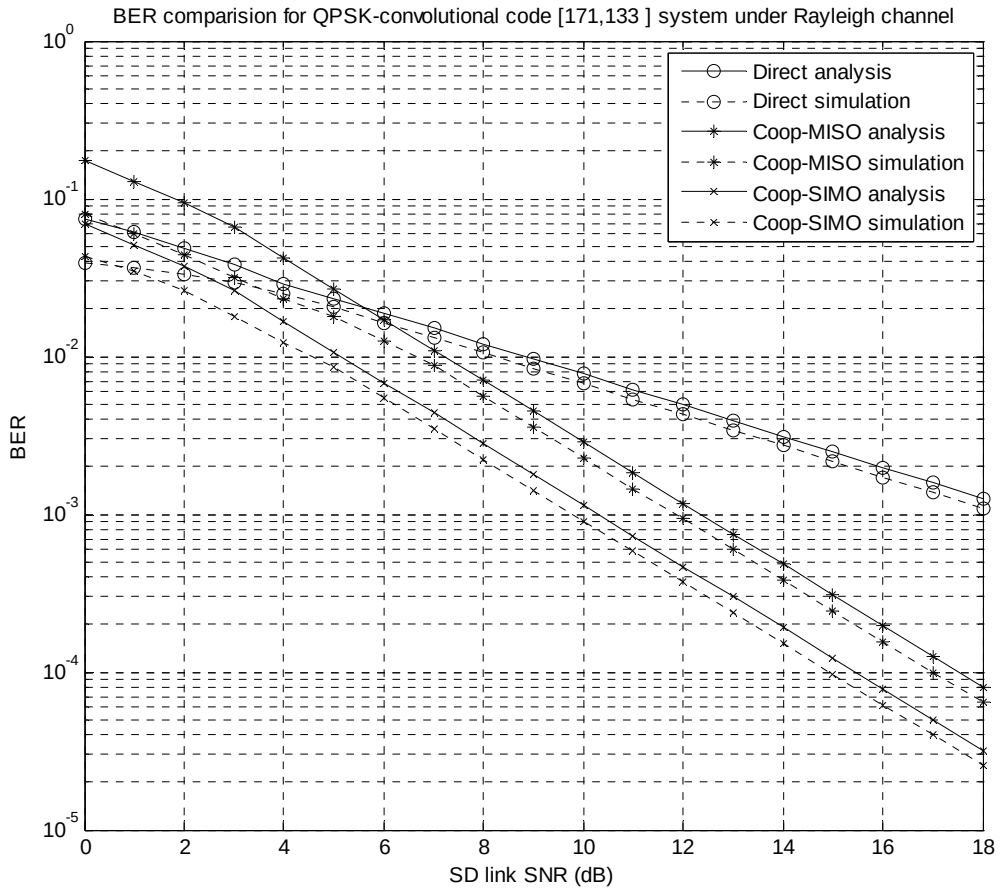

Figure 3-7: BER performance of simulations and bounds of each cooperative diversity scheme

Then, we employ the proposed cooperative diversity schemes in WiMAX OFDM systems. In the following simulations, the symbol time and the subcarrier spacing are

fixed. The CP length is chosen as $T_b/16$ to ensure the maximum delay spread to be smaller than the CP length, and the modulation scheme used here is QPSK. The parameters are based on IEEE 802.16-2005. In the simulation results, BER performance as a function of SNR is evaluated. The SNR is the receive SNR, which is defined as the ratio of the average total signal power received through all the channel paths to the average received noise power. With the consideration of slow mobility, we evaluate the performance under SUI-3 channel mentioned in Chapter 2. Here γ_{SR} is chosen to be 6 dB and γ_{RD} is 8 dB and the relay channel conditions are fixed.

Figure 3-8 and Figure 3-9 show the BER performance of different cooperative diversity schemes with AF based relaying and DF based relaying, respectively. With AF based relaying, both two schemes can achieve better BER performance than direct transmission when the S-D link SNR is below 5 dB, and Coop-SIMO can provide better performance than Coop-MISO, which can achieve nearly 0.5 dB. Because Coop-SIMO can be referred as virtual SIMO system, it can provide additional antenna gain by multiple receive antennas. With DF based relaying, as shown in Figure 3-9, Coop-SIMO can achieve much better BER performance than direct transmission when the S-D link SNR is below 6 dB, but Coop-MISO only can provide better performance when the S-D link SNR is below 5 dB. Comparing Figure 3-8 and Figure 3-9, the simulation results show that DF based relaying can provide better performance than AF based relaying because the relay with DF based relaying can detect and correct some error. Although DF based relaying can provide better performance, the delay time will increase due to the procedure of decoding and encoding. In other words, although the performance of AF based relaying is worse than DF based relaying, the relay can be viewed as a repeater and cause few delay time.

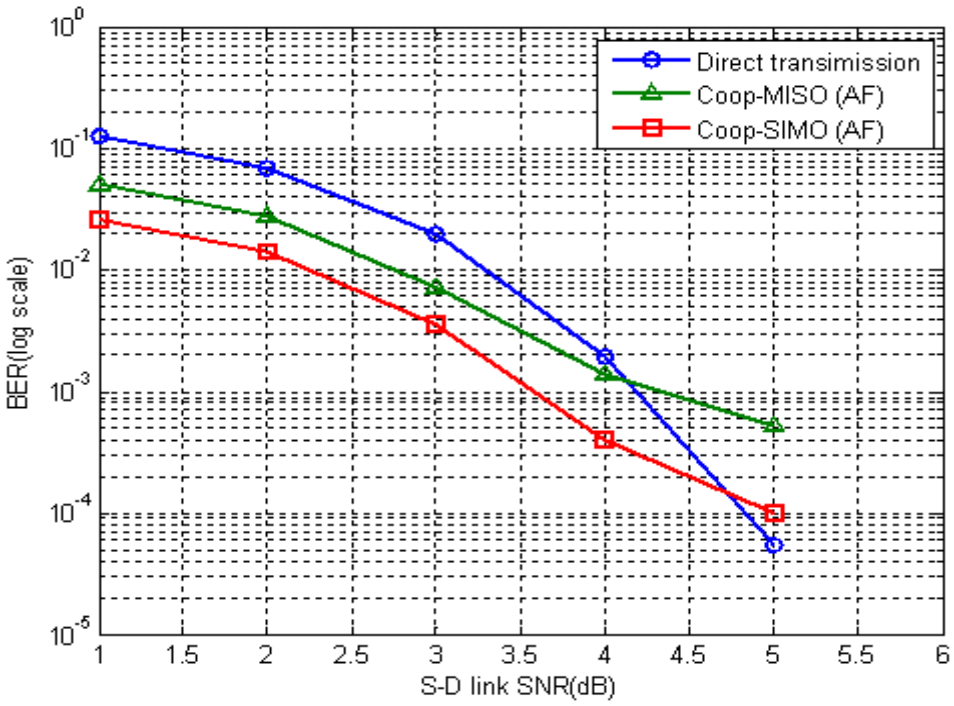

Figure 3-8: BER performance of cooperative diversity schemes with AF based relaying

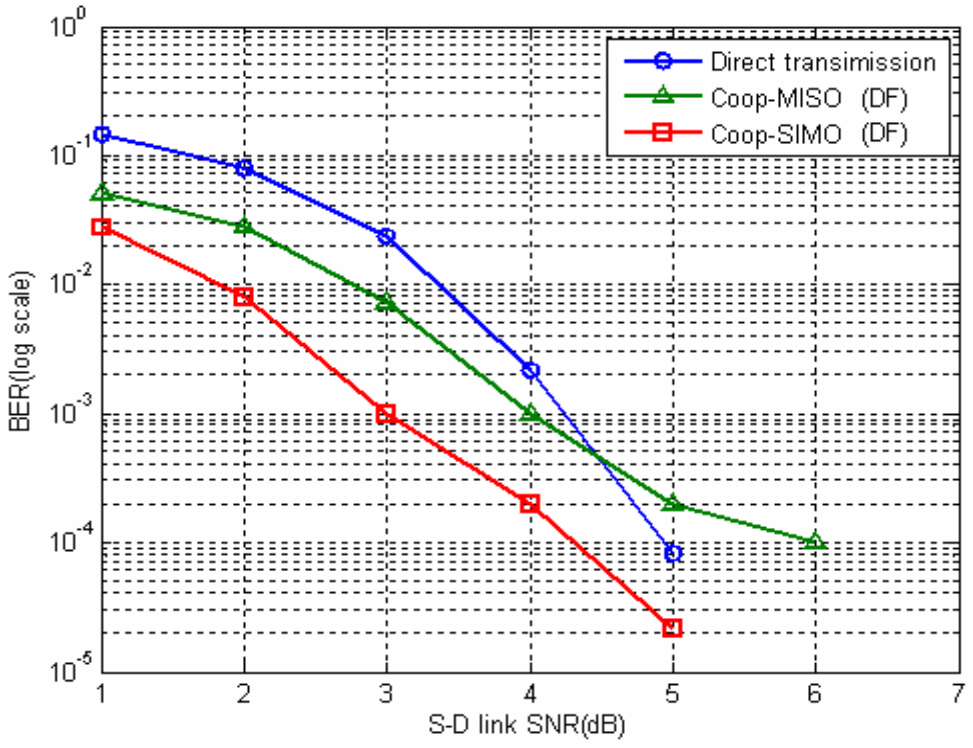

Figure 3-9: BER performance of cooperative diversity schemes with DF based relaying

3.6 Summary

In this chapter, we first propose two cooperative diversity schemes to employ cooperative transmission into wireless networks, and derive the post processing instantaneous SNR at receiver to calculate the capacity of each scheme. Then, the average BER upper bounds are derived by the performance bounds of convolutional codes using the post processing instantaneous SNR. Finally, the structure of transmitter and receiver is proposed to implement each cooperative diversity scheme to WiMAX systems. The computer simulations show the performance of each cooperative diversity scheme and prove that incorporating cooperative transmission in WiMAX systems can improve the performance of the system.

Chapter 4

Modified Cooperative Schemes under AAS and AMC Zones

In wireless communications, AAS and AMC are promising techniques to improve system performance. AAS is generally used to increase system capacity and extend system coverage, and AMC offers an alternative link adaptation method to raise the overall system capacity. Although both AAS and AMC are optional features in WiMAX systems, we still propose to employ the cooperative diversity schemes under AAS and AMC zones to obtain better performance. In this chapter, we modify the cooperative diversity schemes proposed in Chapter 3 to match up the properties of AAS and AMC. Furthermore, in order to raise the end-to-end throughput, a link adaptation method can be designed for the base station to make decision of transmission scheme which can provide the highest throughput.

4.1 AAS for Cooperative Diversity Schemes

Smart antenna technology is one of the most promising technologies for increasing both system coverage and capacity, and is generally termed as the adaptive antenna system (AAS) in WiMAX [24]. Although AAS is an optional feature in WiMAX systems, it can significantly improve range and capacity by adapting the

antenna pattern and concentrating its radiation to each individual user through the use of more than one antenna elements at the base station. In other words, the main purpose of AAS is to generate an adaptive and adjustable antenna beam to maximize the antenna gain in the desired direction and simultaneously place minimal radiation pattern in the directions of the interferers. Generally, these antenna systems of AAS can be classified as either switched-beam antenna system or adaptive antenna array system [25]. A switched-beam antenna system consists of several highly directive, fixed, pre-defined beams, as shown in Figure 4-1. Beams are formed to have high sensitivity in particular fixed directions or sectors. The antenna system detects signal strength and chooses from one of several predetermined and fixed beams. Then, it switches from one beam to another as the user moves throughout the sector. In our study, we propose to employ modified cooperative diversity schemes to a switched-beam antenna system and intend to improve performance.

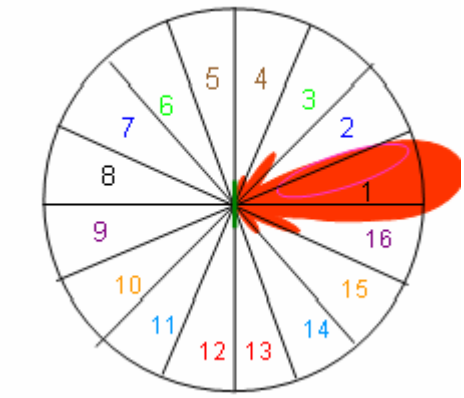

Figure 4-1: Switched beam system

Here we assume that only the base station can work under AAS and DF based relaying is considered, and the two sectors of which the relay and the destination belong to respectively are not adjacent to avoid interference. For Coop-SIMO scheme under AAS, the base station only transmits data during the first time slot and turns to be silent during the second time slot. Therefore, a switched-beam system only needs

to select the beam during the first time slot. We assume that the switched-beam system at the base station can not only choose more than one beam for different directions but also adaptively alter the percentage of the power P_{AAS} which is gained by AAS. Because the base station transmits data to both the relay and the destination, two beams should be chosen: one is the direction of the relay and the other is the direction of the destination, as shown in Figure 4-2. In other words, the base station has to choose two beams which are the direction of the relay and the destination respectively and allocate the power P_{AAS} to the beams which are chosen to transmit.

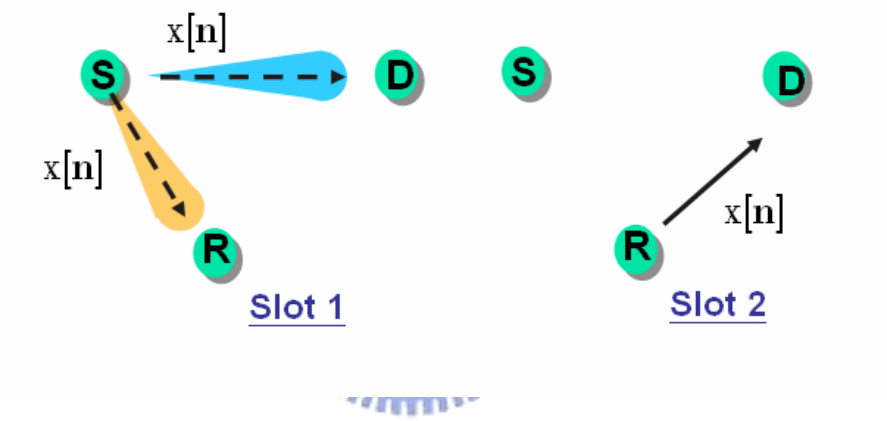

Figure 4-2: Coop-SIMO scheme under AAS

Note that it is possible for the relay to decode symbols in error resulting in error propagation. According to the simulations, when the SNR of the S-R link channel is over 12 dB, the effect of error propagation is relieved. Therefore, we take the instantaneous SNR of S-R link as an indication of the reliability of the relay detection. If the instantaneous SNR of the S-R link is higher than the threshold, the relay can almost decode the data from the base station and the effect of error propagation can be ignored. If the instantaneous SNR of the S-R link is over the threshold ρ (12 dB), because the effect of error propagation is relieved, the base station allocates all the power P_{AAS} to the beam of direct link and the other beam maintains the power

which is the same as no AAS. The power of direct link P_{SD} can be given by

$$P_{SD} = P_{AAS}\,. \tag{4-1}$$

If the instantaneous SNR of S-R link is not over the threshold ρ (12 dB), the effect of error propagation becomes noticeable and affects performance significantly. Therefore, we should first solve the effect of error propagation. In other words, P_{AAS} should be allocated to the direction of the S-R link first and the power of the S-R link P_{SR} can be given by

$$P_{SR} = \rho - \gamma_{SR}\,, \tag{4-2}$$

and the power of S-R link P_{SD} can be given by

$$P_{SD} = P_{AAS} - P_{SR}\,. \tag{4-3}$$

It is easy to implement the Coop-MISO scheme under AAS because of its way of transmission, as shown in Figure 4-3. During time slot 1 and time slot 2 (first phase), the base station transmit data to the relay. Because data only needs to be transmitted to the relay at this phase, the base station can choose the direction of where the relay is and then form the beam. During time slot 3 and time slot 4 (second phase), the base station and the relay transmit space time codes simultaneously. The base station chooses the direction of where the destination is and then forms the beam. In conclusion, incorporating cooperative diversity schemes in a switched-beam antenna system can improve performance by maximizing the antenna gain in the desired direction, and the simulations will be presented in Section 4-4.

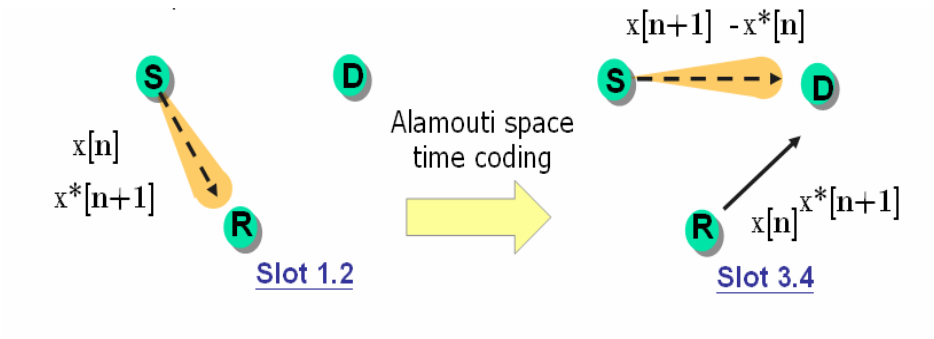

Figure 4-3: Coop-MISO scheme under AAS

4.2 AMC for Cooperative Diversity Schemes

In wireless communication systems, the quality of a signal received by the user depends on several factors: the distance between the destination and the base stations, path loss exponent, shadowing, short term Rayleigh fading and noise. In order to improve system peak data rate, end-to-end throughput and coverage, the signal transmitted to a particular user is modified to account for the signal quality variation through a process commonly referred to as link adaptation. Traditionally, CDMA systems have used fast power control as the preferred method for link adaptation. Recently, AMC have offered an alternative link adaptation method that promises to raise the overall system capacity [26]. AMC provides the flexibility to match the modulation-coding scheme to the average channel conditions for each user. With AMC, the power of the transmitted signal is held constant over a frame interval, and the modulation and coding format is changed to match the current received signal quality or channel conditions. In a system with AMC, users close to the Node B are typically assigned higher order modulation with higher code rates (e.g. 64 QAM with R=3/4 turbo codes), but the modulation-order and/or code rate will decrease as the distance from Node B increases.

Recently, AMC have offered an alternative link adaptation method that promises to raise the overall system capacity. With AMC, the modulation and coding format is changed to match the current received signal quality or channel conditions. Cooperative transmission as mentioned before can significantly increase capacity, as proved by simulations, but end-to-end throughput is bounded according to the specific modulation and coding even if the relay channel condition is very good. Therefore, providing an efficient AMC decision for cooperative diversity schemes based on not only γ_{SD} but also the relay channel γ_{SR} and γ_{RD}.

In order to comply with the constant BER criterion, the threshold for switching between two coding modulation schemes is obtained by drawing horizontal line at the target BER as shown in Figure 4-4. Here we assume that the target BER is 10^{-3}, and the coding and modulation schemes used are mentioned in Chapter 2. Under SUI-3 channel, the vertical lines in Figure 4-4 are the SNR threshold for switching one coding modulation scheme to another when the instantaneous SNR at receiver is over the threshold SNR. In other words, when the instantaneous SNR at receiver is higher than the threshold SNR, we can choose coding modulation scheme which can achieve higher data rate.

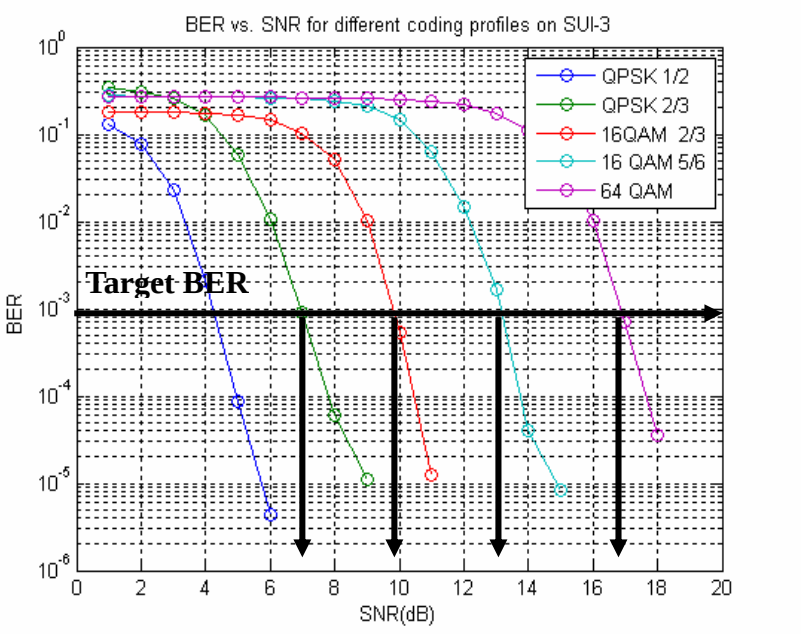

Figure 4-4: BER curves for different coding profiles under SUI-3 channel

The AMC mode decision should take into account the post processing SNR at receiver derived in chapter 3 when employing cooperative diversity schemes. For AF based relaying, the AMC mode decision can be based on the post processing SNR derived before ((3-9) and (3-27)). In other words, the base station calculates the post processing SNR γ^{AF} and makes the AMC mode decision based on γ^{AF}. For

Coop-SIMO AF based relaying, the AMC mode decision should be based on:

$$\gamma_{SIMO}^{AF} = \frac{\left(\gamma_{SD} + \frac{\gamma_{SR}\gamma_{RD}}{1+\gamma_{SR}}\right)^2}{\gamma_{SD} + \frac{\gamma_{SR}\gamma_{RD}}{1+\gamma_{SR}} + \frac{\gamma_{SR}\gamma_{RD}^{\ 2}}{\left(1+\gamma_{SR}\right)^2}}. \tag{4-4}$$

For Coop-MISO AF based relaying, the AMC mode decision should be based on:

$$\gamma_{MISO}^{AF} = \frac{\gamma_{SD} + \frac{\gamma_{SR}\gamma_{RD}}{1+\gamma_{SR}}}{1 + \frac{\gamma_{RD}}{1+\gamma_{SR}}} \tag{4-5}$$

For DF based relaying, the AMC mode decision should take into account the SNR at the relay as the signal needs to be decoded correctly with high probability. For Coop-SIMO scheme, we propose to choose the AMC mode to be used by the base station and the relay based on (4-4)

$$\rho_{SIMO}^{DF} = \min\left\{thr\left(\gamma_{SR}\right), thr\left(\gamma_{SIMO}^{DF}\right)\right\}. \tag{4-6}$$

This is equivalent to $\min\left\{\gamma_{SR}, \gamma_{SIMO}^{DF}\right\}$. If $\rho_{SIMO}^{DF} = thr\left(\gamma_{SR}\right)$, the AMC mode decision is determined by γ_{SR} ; if $\rho_{SIMO}^{DF} = thr\left(\gamma_{SIMO}^{DF}\right)$, the AMC mode decision is determined by γ_{SIMO}^{DF}. For Coop-MISO scheme, it does not necessitate two phases with equal duration because that the destination does not received any signal transmitted in the first phase. That is to say, if the relay channel condition is good enough to choose the better coding modulation scheme, the AMC mode decision of first phase can be determined only by γ_{SR}. Therefore, we adjust the AMC mode decision of Coop-MISO scheme for each phase independently. This leads to an efficient use of radio resource. In other words, for Coop-MISO DF based relaying, the AMC mode decision at first phase should be based on γ_{SR}, and the AMC mode decision at second phase should be based on γ_{MISO}^{DF}.

As we mentioned before, the end-to-end throughput which depends on the nominal rate and the packet error rate can be given as

$$thr(\gamma) = R(\gamma)\big(1 - PER(\gamma)\big). \tag{4-7}$$

We alter the AMC mode decision according to each discrete SNR γ and calculate $thr(\gamma)$ of different SNR γ. Then, we store $thr(\gamma)$ for each discrete SNR γ in the look-up table, as shown in Figure 4-5. With this look-up table, the end-to-end throughput for a given instantaneous SNR γ is determined by reading the corresponding throughput. Furthermore, $thr(\gamma)$ depends on the packets length which is fixed to 96 code bits in our study. For DF based relaying, the end-to-end throughput should be calculated not only by $thr\left(\gamma^{DF}\right)$ and $thr(\gamma_{SR})$ but also $PER(\gamma_{SR})$ and $PER\left(\gamma^{DF}\right)$. Therefore, we should also store $PER(\gamma)$ for each discrete SNR γ as a look-up table.

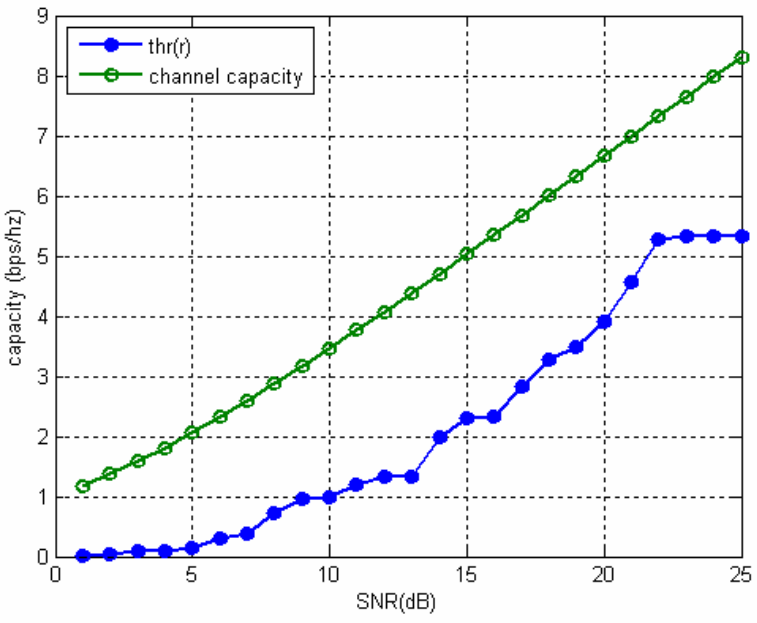

Figure 4-5: Look-up table for stored $thr(\gamma)$

4.3 Proposed Link Adaptation under WiMAX OFDMA AMC Zone

With the observations in the previous section, we propose a link adaptation method for OFDM and OFDMA TDD based wireless relay networks. The proposed link adaptation method is done by the based station. The channel state information regarding the SNR of each subcahnnel of S-D, S-R, and R-D links are reported by the users and then obtained at the base station. The users report the channel state information at the end of each Up-link (UL) subframe via the channel quality indication channel (CQICJ) [11]. Let the channel state information be referred to as $\gamma_{SD,j}$, $\gamma_{SR,j}$, and $\gamma_{RD,j}$ for each subchannel j. Then the base station calculates the post processing SNR for each subchannel to determine the transmission scheme for each subchannel. In other words, because the channel conditions are not the same within the whole bandwidth, different subchannels may use different transmission schemes which provide the highest end-to-end throughput.

Modified frame structure for proposed link adaptation method

Figure 4-6 presents a modified frame structure for employing the proposed link adaptation method in an OFDMA TDD based wireless relay network. In this network, all of the users are in the coverage area of the base station and some of them are in the coverage area of both the relay and the base station. The base station determines the schemes for transmission which has the highest throughput. After finishing the procedure of link adaptation, the base station broadcasts the information of transmission schemes which are used by each subchannel (among direct transmission, AF, and DF) in down link (DL) - MAP. After the first phase and the guard interval for transmit/receive turnaround time, the relay starts to transmit. The relay transmits its

preamble and control information to the users. Finally, the relay and the base station start to transmit in the second phase with the transmission scheme employed for each subchannel. For Coop-MISO DF based relaying, the duration of the first phase can be altered based on the channel conditions of the S-R link.

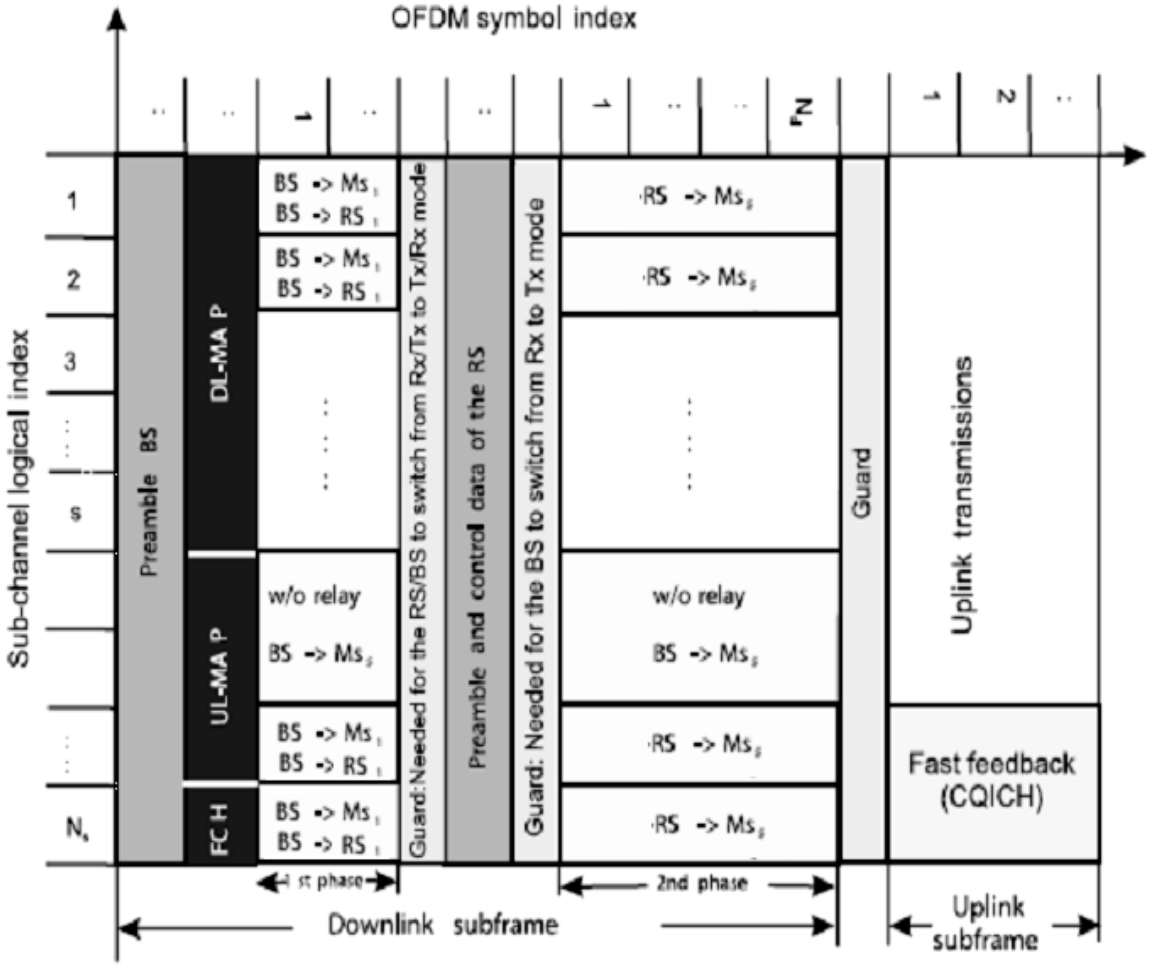

Figure 4-6: Modified frame structure for proposed link adaptation method

Proposed link adaptation method

Figure 4-7 illustrates the flow chart of the link adaptation method we proposed. This link adaptation method is done with the proposed AMC decision mentioned previous and it should be based on two look-up tables mentioned previous: the

look-up tables for $thr(\gamma)$ and $PER(\gamma)$. First, the base station calculates the post processing SNR of three kinds of transmission schemes for each subchannel ($\gamma_{direct,j}$, $\gamma_{AF,j}$, and $\gamma_{DF,j}$) by the CSI obtained via CQICH. Then, the base station reads the look-up tables and uses the equation we derived in chapter 3 to determine the end-to-end throughput of each transmission scheme. Finally, the base station makes the decision of cooperation or not and chooses the transmission scheme which provides highest end-to-end throughput. In WiMAX AMC zone, each subchannel is composed by six bins and each bin is composed by eight subcarriers: one subcarrier for pilot tone and eight subcarriers for data tone. If we calculate the end-to-end throughout of all the subcarriers, this procedure cause a lot of calculation time. Because the channel conditions of adjacent subcarriers are similar, in order to reduce complexity of calculation, the base station calculates the end-to-end throughput for each subchannel only by six pilot subcarriers of each bin. In other words, the end-to-end throughput for each subchannel is determined by six pilot subcarriers of the bins in the same subchannel.

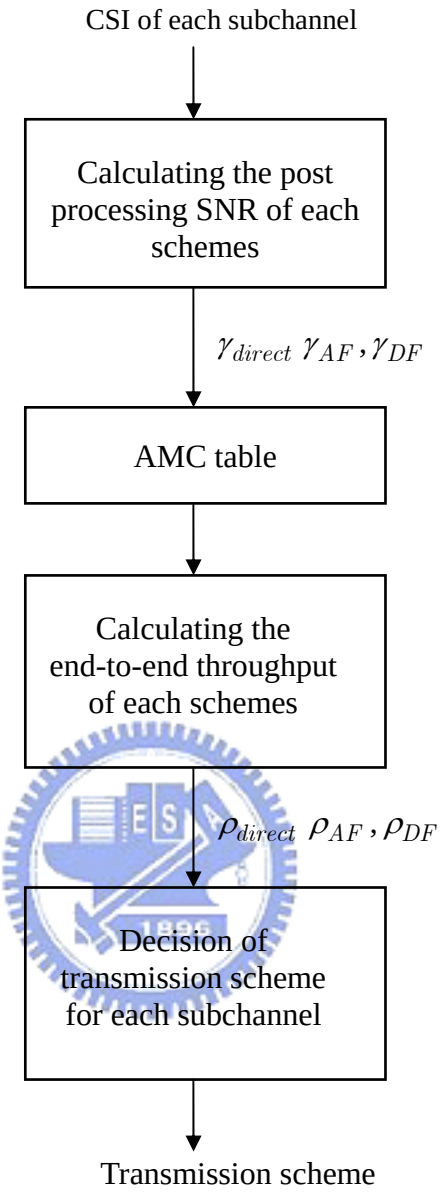

Figure 4-7: Flow chart of proposed link adaptation method

4.4 Computer Simulations

In this section, computer simulations are conducted to evaluate the performance of each cooperative diversity scheme under AAS and AMC zones and the capacity of link adaptation method we proposed. In the following simulations, the symbol time and the subcarrier spacing are fixed. The CP length is chosen as $T_b/16$ to ensure the

maximum delay spread to be smaller than the CP length, and the modulation scheme used here is 16 QAM. Table 4-1 lists all the parameters used in our simulations and the parameters are based on IEEE 802.16-2005.

Table 4-1: Parameters of the simulated system

Parameter	Value
FFT length	1024
Bandwidth (MHz)	10
Sampling frequency (MHz)	11.4
Carrier frequency (GHz)	2.5
Useful Symbol Time T_b (μs)	89.6
Guard Interval (μs)	11.2
Subchannel Mode	PUSC
Modulation	16 QAM
Code rate	1/2

In the simulation results, BER performance as a function of SNR is evaluated. The SNR is the receive SNR, which is defined as the ratio of the average total signal power received through all the channel paths to the average received noise power. With the consideration of slow mobility, we evaluate the performance under SUI-3 channel mentioned in Chapter 2.

To see that cooperative diversity schemes under AAS can improve performance of the system, we compare the BER performance between each cooperative diversity

scheme with and without AAS in Figure 4-8 and Figure 4-9. Here γ_{SR} is chosen to be 8 dB and γ_{RD} is 12 dB and the relay channel conditions are fixed. Figure 4-8 and Figure 4-9 show that BER performance of Coop-MISO and Coop-SIMO under AAS, and both direct transmission and Coop-MISO can achieve additional gain by AAS. The simulation results confirm that the modified cooperative diversity schemes can provide better performance than direct transmission under AAS. Furthermore, the modified Coop-SIMO scheme under AAS can achieve better performance than the scheme which we allocate equal power to both the S-D link and S-R link, as shown in Figure 4-9. Therefore, the simulation results ascertain that both the modified Coop-MISO and Coop-SIMO schemes can improve the performance under AAS comparing with direct transmission.

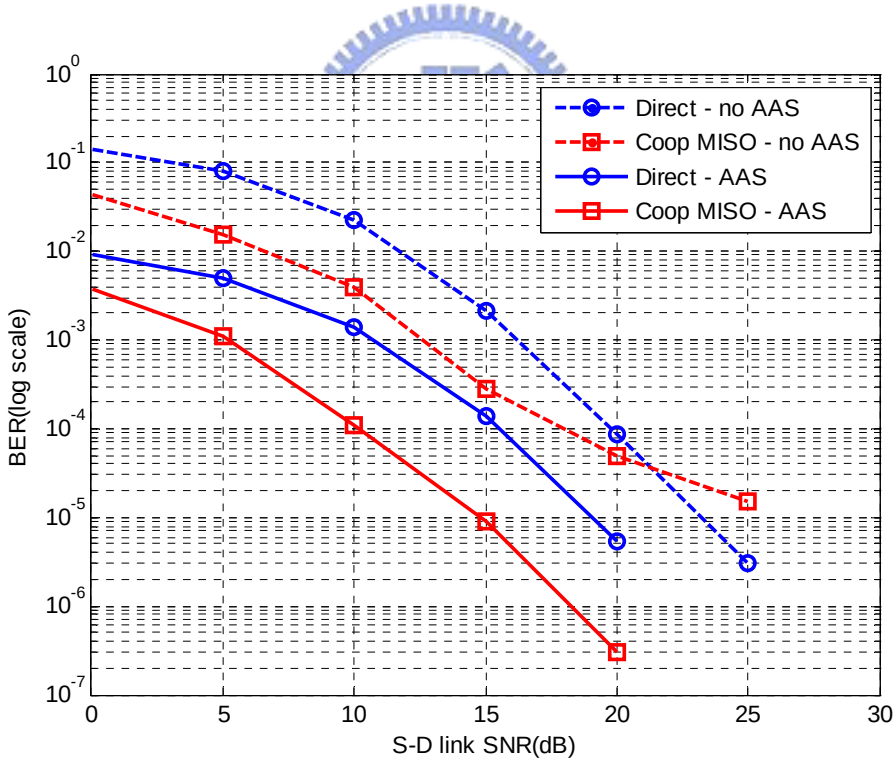

Figure 4-8: BER performance of Coop-MISO scheme with and without AAS

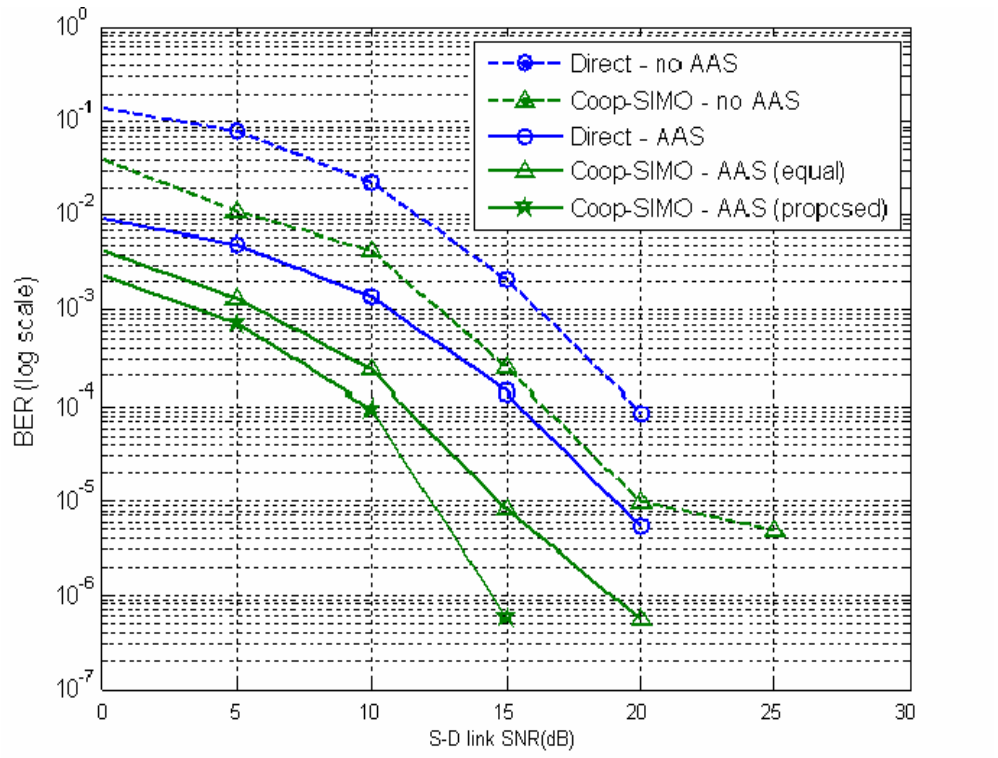

Figure 4-9: BER performance of Coop-SIMO scheme with and without AAS

To see that cooperative diversity schemes under AMC can improve the end-to-end throughput of the system, we compare different conditions of the relay channel γ_{SR} and γ_{RD} in Figure 4-10. The parameters are the same as Table 4-1 except for the subchannel mode. Here AMC allocation is used in subchannel mode and Coop-SIMO scheme is employed, and horizontal axis represents the instantaneous SNR of S-R link and vertical axis represents the capacity (b/s/Hz). As we mentioned previously, the end-to-end throughput is bounded according to the specific modulation and coding even if the relay channel condition is very good. The results in this figure show that, as the relay conditions become better, the post processing SNR at receiver will change according to the equation derived before and the decision of AMC scheme will also alter according to the post processing SNR. Furthermore, in the figure, we can see that there is a jump of the capacity when the SNR of S-R link changes from 6 dB to 7 dB. The appearance is because that the

decision of AMC scheme is changed to another specific code and modulation according to the post processing SNR. In conclusions, if we employ cooperative diversity schemes under AMC zone and make AMC decision based on γ_{SD}, γ_{SR}, and γ_{RD}, the end-to-end throughput is improved when the relay channel is good.

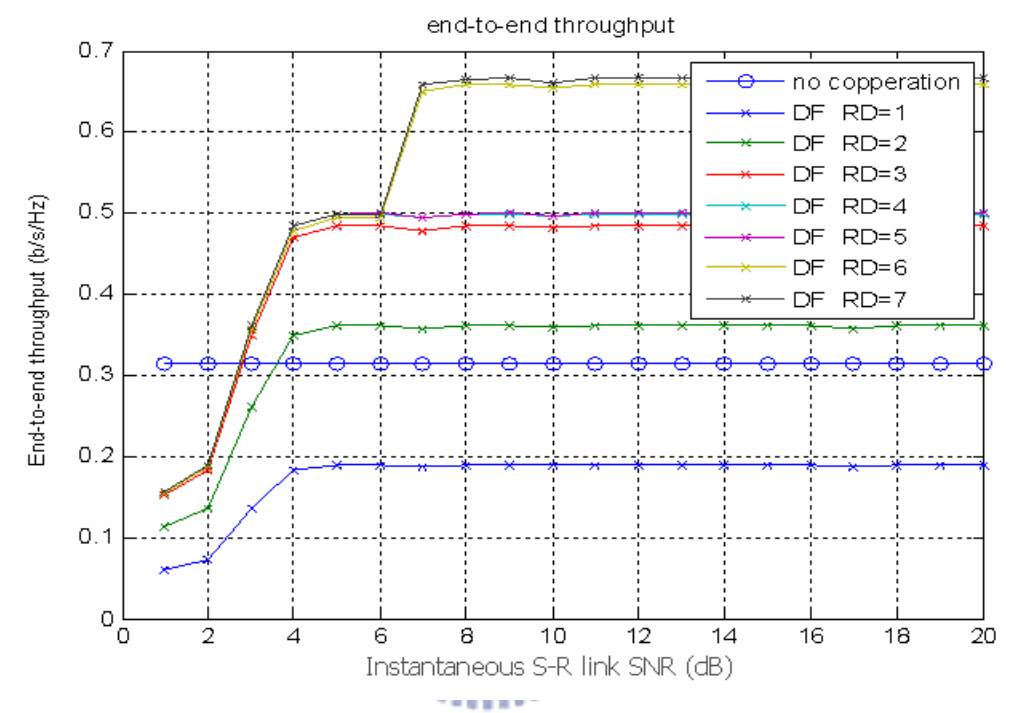

Figure 4-10: End-to-end throughput under different conditions of relay channel

At last, the end-to-end throughput of the proposed link adaptation method is shown in Figure 4-11. The figure presents the end-to-end throughput not only of the proposed link adaptation method but also of the AF based relaying, DF based relaying, and direct transmission. The schemes of cooperative schemes with AF based relaying and DF based relaying and direct transmission scheme are used in all the subchannels. For the Coop-SIMO scheme, the results in Figure 4-11 are obtained versus the average SNR condition in the S-R link where the average SNR conditions in the S-D link and the R-D link are fixed at 5 dB and 9 dB. The figure shows that the average end-to-end throughput performance obtained by the proposed link adaptation method

is always better than or equal to other schemes. As the SNR of S-R link is between 0 dB and 6 dB, the throughput of the proposed link adaptation method is the same as the direct transmission because the relay channel condition is not good enough to employ cooperative diversity scheme. Therefore, the direct transmission is chosen by the base station in this case. As the SNR of the S-R link is over 7 dB, some subchannels are employ cooperative scheme with DF based relaying due to that the relay channel gets better. When the SNR of S-R link is over 16 dB, all the subchannels are employed cooperative scheme with DF based relaying and the average end-to-end throughput of the proposed link adaptation method is the same as the cooperative scheme with DF based relaying. Because cooperative scheme is chosen only when it can provide a higher throughput, the simple selection scheme for cooperative transmission based on OFDMA-TDD networks can be proposed to ensure that the average end-to-end throughput is always better than or equal to that of transmissions without relay.

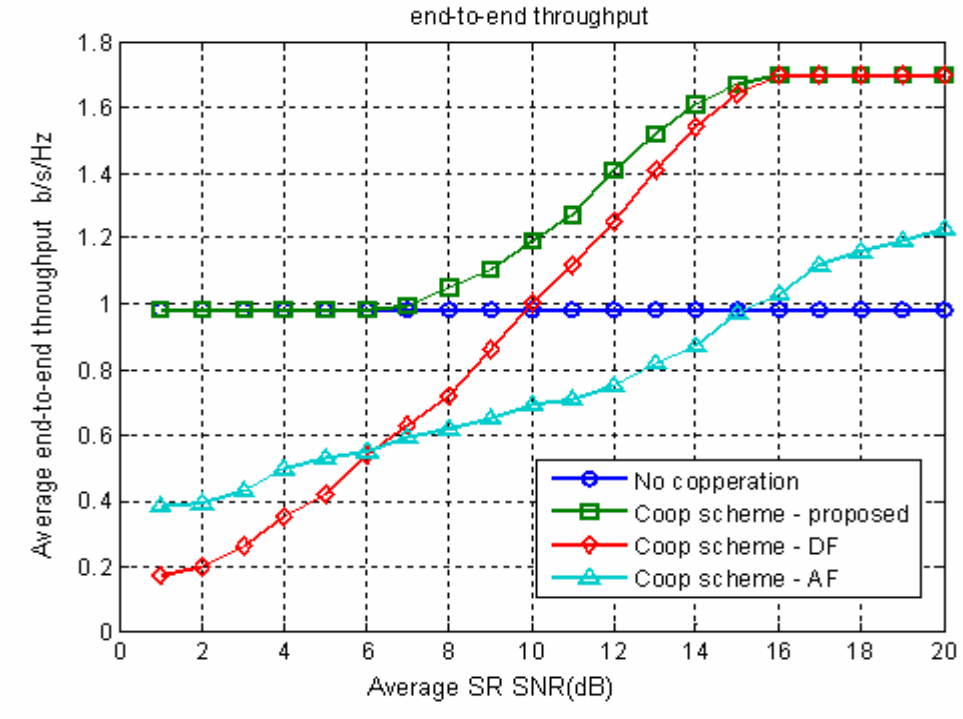

Figure 4-11: End-to-end throughput of proposed link adaptation method

4.5 Summary

In this chapter, we first incorporate the cooperative diversity scheme in AAS and modify the cooperative schemes under AAS to improve the performance. Then, we discuss how to make the AMC decision when cooperative diversity schemes are used under AMC zone. The modified cooperative diversity schemes under AAS and AMC are introduced in detail. At last, a simple link adaptation method is proposed to ensure that the average end-to-end throughput is always better or equal to direct transmission. Computer simulation results show that the proposed scheme under the IEEE 802.16-2005 standard can effectively improve the performance of the system.

Chapter 5

Conclusion

In this thesis, we propose two cooperative diversity schemes to incorporate cooperative transmission in OFDM(A) based systems. By deriving the post processing instantaneous SNR, we can evaluate the throughput of each cooperative diversity scheme and confirm that cooperative diversity schemes can improve both the BER and the throughput of the system. Also, the system is constructed following the OFDMA mode in the IEEE 802.16-2005 standard and is proven to be effective by simulations in slow mobility environment.

In Chapter 2, the transmitter architecture and specification of IEEE 802.16-2005 system have been introduced. We also introduce the multiple-antenna transmit techniques such as STC and AAS adopted in the standard. In the rest of this chapter, we introduce the SUI channel model from the fixed wireless channel environment.

In Chapter 3, two cooperative diversity schemes are proposed: Coop-MISO scheme and Coop-SIMO scheme. We derive the post processing instantaneous SNR and calculate the end-to-end throughput of each scheme. The two cooperative schemes can provide both higher end-to-end throughput and better BER performance than direct transmission when the relay channel conditions are good. Furthermore, the Coop-SIMO scheme can provide better performance than the Coop-MISO scheme due to additional antenna gain. We also derive the average BER upper bounds by the

BER performance upper bound of convolutional codes. At last, we propose two structures of transmitter and receiver to implement the Coop-MISO scheme and Coop-SIMO scheme in WiMAX systems respectively, which is following the IEEE 802.16-2005 standard. The simulations results confirm that incorporating cooperative diversity in WiMAX OFDM(A) systems can significantly improve both the BER performance and the end-to-end throughput of the system.

In Chapter 4, we introduce two optional features in WiMAX systems: AAS and AMC. In order to improve the performance of cooperative transmission, we modify two cooperative diversity schemes proposed in Chapter 3 to match up the properties of AAS and AMC, and the improvement of modified cooperative diversity schemes under AAS and AMC can be shown by computer simulations. Finally, a simple link adaptation method is proposed for the base station to make the decision of which transmission scheme is adopted. The simulations results show that the proposed link adaptation method can ensure that the end-to-end throughput is always better or equal to direct transmission.

Since there has been growing interest in the integration of cooperation into conventional wireless networks, the major contribution of this thesis is that the proposed cooperative diversity schemes and link adaptation method can confirm the improvement of the system performance. In our case, the cooperative diversity schemes only confirm the improvement in slow mobility. Future works out of our study can be the design of the proposed link adaptation method for users with high mobility.

Bibliography

[1] *IEEE Std 802.16e-2005 and IEEE Std 802.16-2004/Cor 1-2005*, "Part 16: air interface for fixed and mobile broadband wireless access systems," Feb. 2006.

[2] *IEEE Std 802.16-2004*, "Part 16: air interface for fixed broadband wireless access systems," Oct. 2004.

[3] J. A. C. Bingham, "Multicarrier modulation for data transmission: An idea whose time has come," *IEEE Commun. Mag.*, vol. 28, no. 5, pp. 5-14, May. 1990.

[4] A. Sendonaris, E. Erkip and B. Aazhang, "User cooperation diversity – Part II: implementation aspects and performance analysis," *IEEE Trans. Commun.*, vol. 51, no. 11, pp. 1939-1948, Nov. 2003.

[5] J. M. Laneman, G. W. Wornell, and D. N. C.. Tse, "Cooperative diversity in wireless networks: efficient protocols and outage behavior," *IEEE Trans. Inf. Theory*, vol. 50, no. 12, pp. 3062-3080, Dec. 2004.

[6] J. M. Laneman, G. W. Wornell, and D. N. C.. Tse, "Distributed space-time-coded protocols for exploiting cooperative diversity in wireless networks," *IEEE Trans. Inf. Theory*, vol. 49, no. 10, pp. 2415-2425, Oct. 2003.

[7] A. Nosratinaia, T. E. Hunter, and A. Hedayat, "Cooperative communication in wireless networks," *IEEE Commun. Mag.*, vol. 42, no. 10, pp. 74-80, Oct. 2004.

[8] A. Stefanov and E. Erkip, "Cooperative coding for wireless networks," *IEEE Trans. Commun.*, vol. 52, no. 9, pp. 1470-1476, Sept. 2004.

[9] R. Pabst, B. H. Walke, D. C. Schultz, P. Herhold, H. Yanikomeroglu, S. Mukherjee, H. Viswanathan, M, Lott, W. Zirwas, M. Dohler, H. Aghvami, D. D. Falconer, and G. P. Fettweis, "Relay-based deployment concepts for wireless and mobile broadband radio," *IEEE Commun. Mag.*, vol. 42, no. 9, pp. 80-89, Sept. 2004.

[10] "Mobile WiMAX - part 1: a technical overview and performance evaluation," *WiMAX Forum*, Feb. 2006.

[11] "Mobile WiMAX - part 2: a comparative analysis," *WiMAX Forum*, April 2006.

[12] A. Salvekar, S. Sandhu, Q. Li, M. Vuong and X. Qian, "Multiple-antenna technology in WiMAX systems," *Intel Technology Journal*, vol. 8, Aug. 2004.

[13] S. Alamouti, "A simple transmit diversity technique for wireless communications," *IEEE J. Sel. Areas Commun.*, vol. 16, no. 8, pp. 1451-1458, Oct. 1998.

[14] *IEEE 802.16a-03/01*, "Channel models for fixed wireless applications," June 2003.

[15] A. Bletasas and A.Lippman, "Efficient Collaborative (Viral) Communication in OFDM Based WLANs," *Inter. Symposium on Advanced Radio Technologies (ISART 2003)*, Boulder Colorado, March 4-7, 2003

[16] S. Yatawatta and A.P. Petropulu, "A Multiuser OFDM System with User Cooperation," *38th Asilonmar Asilonmar Conf. on Signals, Systems, and Computers*, vol.1, pp. 319-323, Nov. 2004

[17] J. N. Laneman, D. N. C. Tse, and G. W. Wornell, "User cooperation diversity-part I: system description," *IEEE Trans. Commun.*, vol. 51, no. 11, pp. 1927-1938, Nov. 2003.

[18] A.Paulraj, R. U. Nabar, and D. Gore, *Introduction to Space-Time Wireless Communications*. Cambridge University Press, 2003.

[19] B. Can, H. Yomo, and E. De Carvalho, “Hybird forwarding scheme for cooperative relaying in OFDM based networks,” in *Proc. IEEE ICC*, lstanbul, Turkey, June 2006.

[20] R.U, Nabar, H. bolcskei, and F. W. kneubuhler, “Fading relay channels: Performance limits and space-time signal design,” *IEEE J. Sel. Areas Commun.*, vol. 22, no. 6, pp. 1099-1109, Aug. 2004.

[21] S. M. Alamouti, “A simple transmit diversity technique for wireless communications,” *IEEE J. Sel. Areas Commun.*, vol. 16, no. 8, pp. 1451-1458, Oct. 1998.

[22] Shu Lin. Daniel J. Costello, Error Control Coding. Person Education, Inc. 2004.

[23] J. G. Proakis, Digital Communications. McGraw-Hill, 2001.

[24] Per H. Lehne, et. al. “An Overview of smart antenna technology for mobile communication systems”. *IEEE Communications, Surveys*

[25] Mohammad Elmusrati, “The smart antenna application in mobile communications,” Helsinki University of Technology, Control Engineering Lab., Lecture Notes, 2002

[26] A. J. Goldsmith and S. G. Chua, “Adaptive Coded Modulation for Fading Channels,” *IEEE Trans. Commun.*, vol. 45, no. 12, pp. 595-602, May 1998